

UC Berkeley

UC Berkeley Previously Published Works

Title

Electric field control of magnetism: multiferroics and magnetoelectrics

Permalink

<https://escholarship.org/uc/item/83b4t32f>

Journal

La Rivista del Nuovo Cimento, 44(5)

ISSN

0393-697X

Authors

Ramesh, R

Martin, LW

Publication Date

2021-05-01

DOI

10.1007/s40766-021-00019-6

Peer reviewed

Electric Field Control of Magnetism – Multiferroics and Magnetoelectrics

R. Ramesh^{1,2,3} & L. W. Martin^{2,3}

¹ Department of Physics, University of California, Berkeley

² Department of Materials Science and Engineering, University of California, Berkeley

³ Materials Sciences Division, Lawrence Berkeley National Laboratory

Table of Contents

I.	Summary	3
II.	Introduction:	3
	II.1 The Macro-systems Perspective	3
	II.2 The need for a new paradigm:	5
	II.3 Energy Efficiency in Computing	6
	II.4 The Opportunity	7
	II.5 The Key Role of Energy Consumption	8
III.	Multiferroics and Magnetoelectrics	10
	III.1 Symmetry and Fundamentals of Magnetoelectric Coupling	11
	III.2 Multiferroic and Magnetoelectric Materials	11
	III.3 Pathways to Create Multiferroic and Magnetoelectric Materials	12
	III.4 Bismuth ferrite as a model multiferroic	13
	III.5 Chemical Substitutions in Bismuth Ferrite	16
	III.6 Chemical and Elastic Phase Equilibria	17
	III.7 Other Physical Phenomena	19
	III.8 Theoretical Studies	20
	III.9 Domains and Domain Walls in Multiferroics	21
IV.	Magnetoelectric Coupling	24
	IV.1 Magnetoelectric Coupling and Heterostructures	24
	IV.2 E- field control of mixed magnetic states and nanocomposites	29
	IV.3 Electric-field control of magnetic orientation through interfacial exchange coupling	31
	IV.4 Electric-field control of magnetic state	33
V.	Ultra-low Power Logic-Memory Devices based on Multiferroics	34
VI.	High frequency applications	38
VII.	Challenges and Opportunities	38
VIII.	Acknowledgements	41
IX.	References	42

I. Summary: This article is written on behalf of a large number of colleagues, collaborators, and researchers in the field of complex oxides as well as current and former students and postdocs who continue to enable and undertake cutting-edge research in the field of multiferroics, magnetoelectrics, and the pursuit of electric-field control of magnetism. What we present is something that is extremely exciting from both a fundamental science and applications perspective and has the potential to revolutionize our world. Needless to say, to realize this potential will require numerous new innovations, both in the fundamental science arena as well as translating these scientific discoveries into real applications. Thus, this article will attempt to bridge the gap between fundamental condensed-matter physics and the actual manifestations of the physical concepts into real-life applications. We hope this article will help spur more translational research within the broad materials physics community.

II. Introduction:

II.1 The Macro-systems Perspective: We begin the discussion from a broad, macro-systems perspective. Microelectronics components and systems form an ever-increasing backbone of our society. Computing devices have pervaded many parts of our daily life, for example through a host of consumer electronics systems, providing sensing, actuation, communication, and processing and storage of information. All of these are built upon an approximately \$470B (US)/year global market that is growing at a steady pace of 10-15% annually^{1,2}. Many of these innovations started as materials physics research ideas, often times first discussed within the hallways of the many physics and materials conferences worldwide. While these applications are essential to our daily lives, all of these will pale into the background with the emergence of a few new global phenomena. The first among them is the notion of the “Internet of Things” (IoT), which is the network of physical devices, vehicles, home appliances, and other items embedded with electronics, software, sensors, actuators, and connectivity which direct integration of the physical world into computer-based

systems, resulting in efficiency improvements, economic benefits, and reduced human exertion³, illustrated schematically in Fig. 1⁴. Thus, it is not inconceivable that every modern building will be outfitted with millions of sensors and actuators that can dynamically optimize the energy consumption dynamics of that building. Similarly, a modern automobile has a large number of sensing, communicating components embedded. While still in its infancy, it is possible that driverless automobiles, for example, will be a routine aspect of our life twenty years from now.

The second major phenomenon is the field of machine learning (ML) / artificial intelligence (AI), that is taking the technology world by storm. It uses a large amount of statistical data analytics which, in turn, provides the computing system the ability to “learn” and do things better as they learn, not unlike normal human beings. While there are several scientific disciplines that come into play, of relevance to us is the fact that microelectronic components are critical underpinnings for this field.

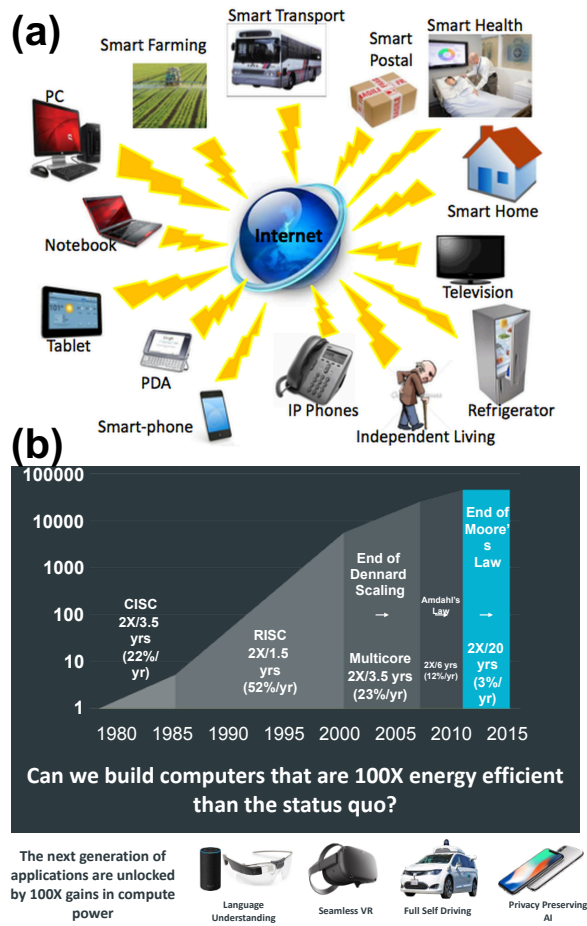


Fig.1: (a) A schematic illustrating the emergence of the “Internet of Things” and Machine Learning/ Artificial Intelligence as macro-scale drivers for the Beyond Moore’s Law R&D [4]. (b) Describes the leveling off of the various scaling laws as a function of time, leading to the end of Moore’s Law.

II.2 The need for a new paradigm: We can now ask the question: how do these global phenomena relate to microelectronics and, more importantly, to new materials? Or stated in a different way, what can *materials physics* do to enable this coming paradigm shift? To put this into perspective, we now need to look at the fundamental techno-economic framework that has been driving the microelectronic field for more than five decades. This is the well-known “Moore’s Law”, which

(a) A new physical phenomenon is needed

Every ~ 20 years a computing revolution is launched by a **physics & materials** driven 100x improvement in energy consumption.

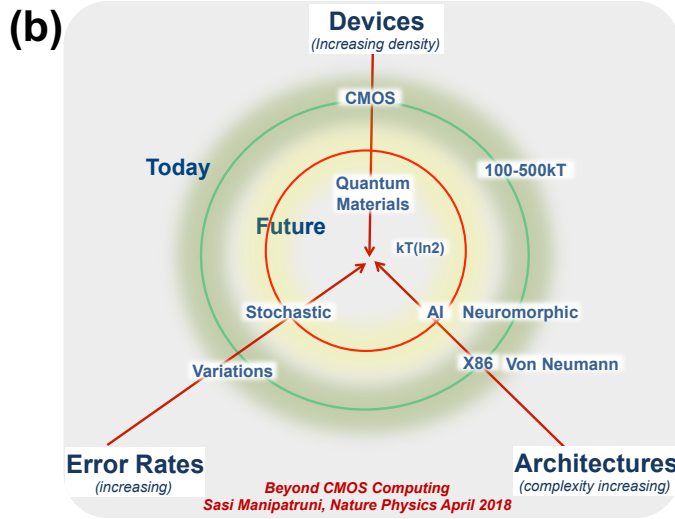
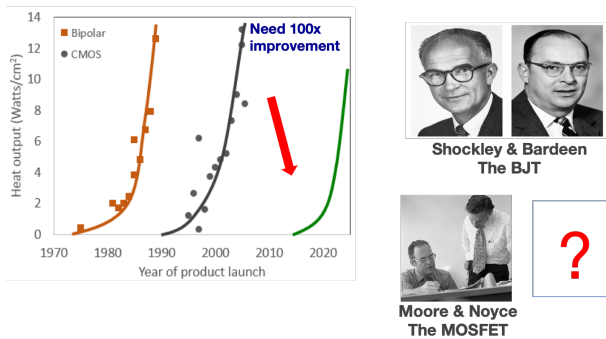


Figure 2: (a) captures the evolution of semiconductor electronics, from Bipolar to CMOS. As the technology has evolved, so has the heat output from the technology, which then leads to a new technology base. These innovations came from Shockley, Bardeen and the Moore and Noyce; the question mark poses the challenge: what comes after this; (b) presents three complementary pathways for Beyond CMOS electronics [1].

underpins the field of microelectronics through the scaling of CMOS-based transistors (Fig. 2). Broadly, it states that the critical dimensions of the CMOS transistor shrink by 50% every 18-24 months. At its inception, CMOS transistors were “macroscopic” with the critical gate dimension well over 1 μm. In 1974, a path to shrinking such transistors, while keeping the power density constant, was proposed^{5,67} and was followed for the next 30+ years. Today, however, so-called Dennard scaling is no longer possible and the critical dimensions of modern transistors are

rapidly approaching sub-10 nm scales; the point at which both the fundamental science (*i.e.*, classical electron dynamics) no longer more suffices to adequately

understand operation and ever more complex manufacturing issues must be addressed. In particular in the past 5-8 years, there has been an ever-increasing sense that something has to be done about this issue^{8,9,10,11,12}.

IT Challenge & Opportunity : Moore’s Law, IoT & AI
Market size ~ \$470B in 2019; growing rapidly

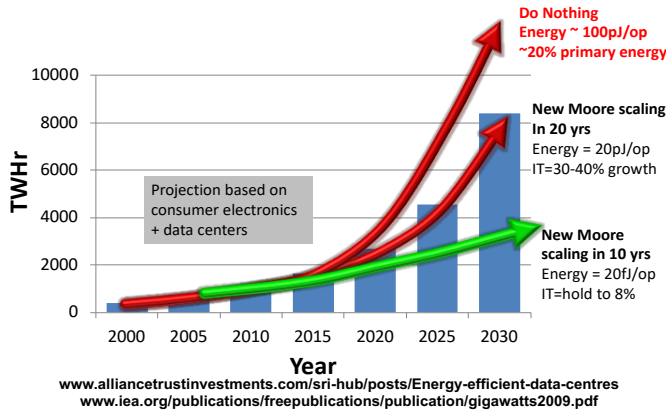


Fig.3: Estimation of the total energy consumed in all of Microelectronics by 2030, if nothing is done to reduce the energy consumption/operation from the ~100pJ/operation level, while the number of microelectronic components is growing exponentially due to the emergence of the “Internet of Things” and Artificial Intelligence/Machine Learning (RED curves). A New Moore’s Law at 20 femtoJoule/operation (GREEN curve) will enable us to keep the energy consumption level at the ~8% level. [13]

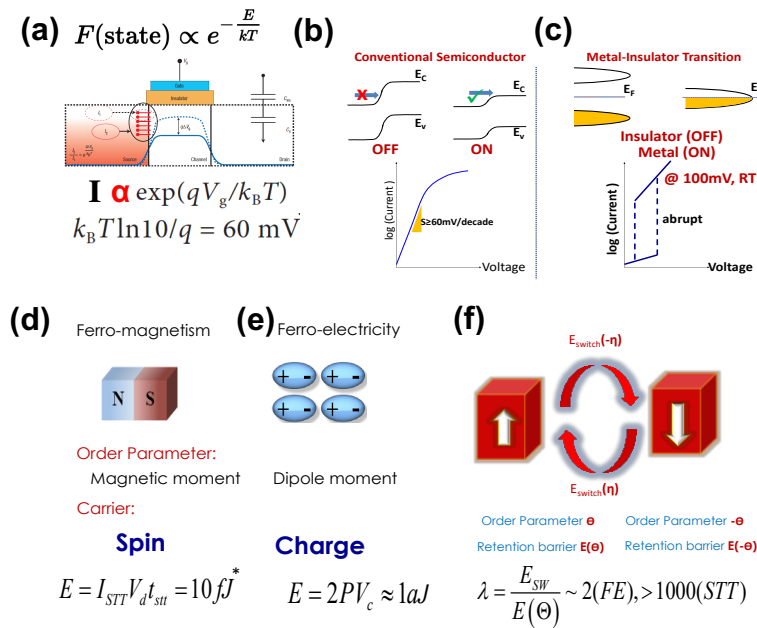
II.3 Energy Efficiency in Computing:

As if this combination of challenges was not enough, we have yet to introduce perhaps the single most important aspect into consideration: energy consumption (Fig. 3)¹³. Of the many issues modern technologists must address, the one we highlight here has the potential to be the most impactful geo-politically and socio-economically: energy. The energy consumed per logic

operation, which in today’s CMOS transistor is of the order of 50-100 pJ/logic operation (note that this actual number may be debated, but it remains that the energy consumed is of the order of pJ/operation). For the sake of discussion, assume that there is no change to this number in the near future, but, all the while, the demand for and consumption of microelectronic components in IoT and AI/ML will grow exponentially. As a consequence, it is quite conceivable that the total energy consumption in all of microelectronics could grow to ~20% of primary energy by 2030¹⁴. For example, it is projected that a single, next-generation exascale supercomputer will consume 5–10% of the total power output from the average coal-fired power plant.¹⁵ Today, it is of the order of 5% and thus is not of great concern, especially in contrast to sectors such as buildings, which consume ~38% of the total energy consumption, or transportation which consumes ~24% (fractions noted here

are for the United States). At the scale of $\sim 20\%$ of primary energy, microelectronics would become a serious component of the worldwide energy consumption mix and thus deserves to be addressed from the energy efficiency perspective as well. Thus, these three global phenomena, namely the emergence of IoT and AI/ML as well as the end of Moore's Law (including aspects of dimensional constraints and total energy consumption in microelectronics) forms the backdrop for our discussion as we ask: **what can we do with new materials physics?**

II.4 The Opportunity: We begin the exploration of new materials by going back to



the fundamentals of CMOS devices, namely the behavior of the electron within the CMOS transistor. The microscopic behavior of the electronic charge is governed by the Boltzmann distribution (Fig. 4)¹⁶. Quick analysis shows that the current changes exponentially with voltage, with a slope of 60

Figure 4: (a) schematically describes the Boltzmann distribution function for electrons in the CMOS channel, leading to the 60mV/decade of current as the limit, which is known as the “Boltzmann Tyranny”, shown in (b) [16]); (c) is a possible manifestation of metal-insulator transition as the base for the next generation of logic; (d,e) describe the emergence of correlations (spin in (d) and dipolar in (e)) that can then be used to reduce the energy consumption in a memory-logic device; (f) schematically describes the ratio of the energy required to switch a ferroelectric element compared to the barrier height.[1].

mV/decade of current¹⁷. Macroscopically, this manifests itself as an I_d - V_g plot with a slope of 60mV/decade, under ideal conditions. This result is termed as the “Boltzmann Tyranny”^{1,11} since the Boltzmann physics is imposed on the functioning of the actual device, very much like a “tyrant” imposes his/her will on the common

masses. To make things worse, in real transistors, this voltage slope can be larger. This fundamental behavior is central to the performance of the transistor, both in terms of the voltage required and the energy consumed in the process of operating the transistor. In recent years, there has been the realization that the Boltzmann Tyranny needs to be addressed – enter the need for new materials. One proposed pathway is to use materials exhibiting a metal-to-insulator transition, such as in correlated-electron systems. Under ideal conditions, such a metal-to-insulator transition can be very abrupt. Another key realization, which is described in a recent review¹, identifies the broad class of quantum materials as possible candidates to overcome this tyranny, mainly through the insertion of an additional, internal interaction energies into the Boltzmann distribution. For example, this could be the exchange interaction in a ferromagnet or the dipolar interaction in ferroelectrics. In its simplest form, such an interaction can be represented by an additional term in the Hamiltonian that represents the exchange interaction energy for a magnet given by: $E_{ex} = -J \cdot S_1 \cdot S_2$, where J is the exchange integral and S_1 and S_2 are the two neighboring spins (or the corresponding dipolar energy in the case of a ferroelectric). Depending on the sign of J , S_1 and S_2 are either parallel (ferromagnet) or antiparallel (antiferromagnet). This term then becomes the key component within the Boltzmann distribution function and it modifies the energy landscape. In simpler terms, the exchange energy (or the dipolar energy in a ferroelectric) makes the spins (or the dipoles) align collectively *without the need* for an external source of energy (such as an applied field). Thus, if one could use spin as the primary order parameter rather than merely charge in a CMOS device, one could take advantage of such internal collective order to reduce the energy consumption. Indeed, this is the premise behind two recent research articles^{1,10}, where the rudiments of a possible magneto-electric spin orbit (MESO) coupled memory-logic device are discussed. While many parts of this device require further detailed study and innovations, one aspect that we will focus on, pertains to electric-field control of magnetism.

II.5 Electric-field Control of Magnetism – The Key Role of Energy Consumption:

We can begin this discussion with a question: why would one use an electric field to

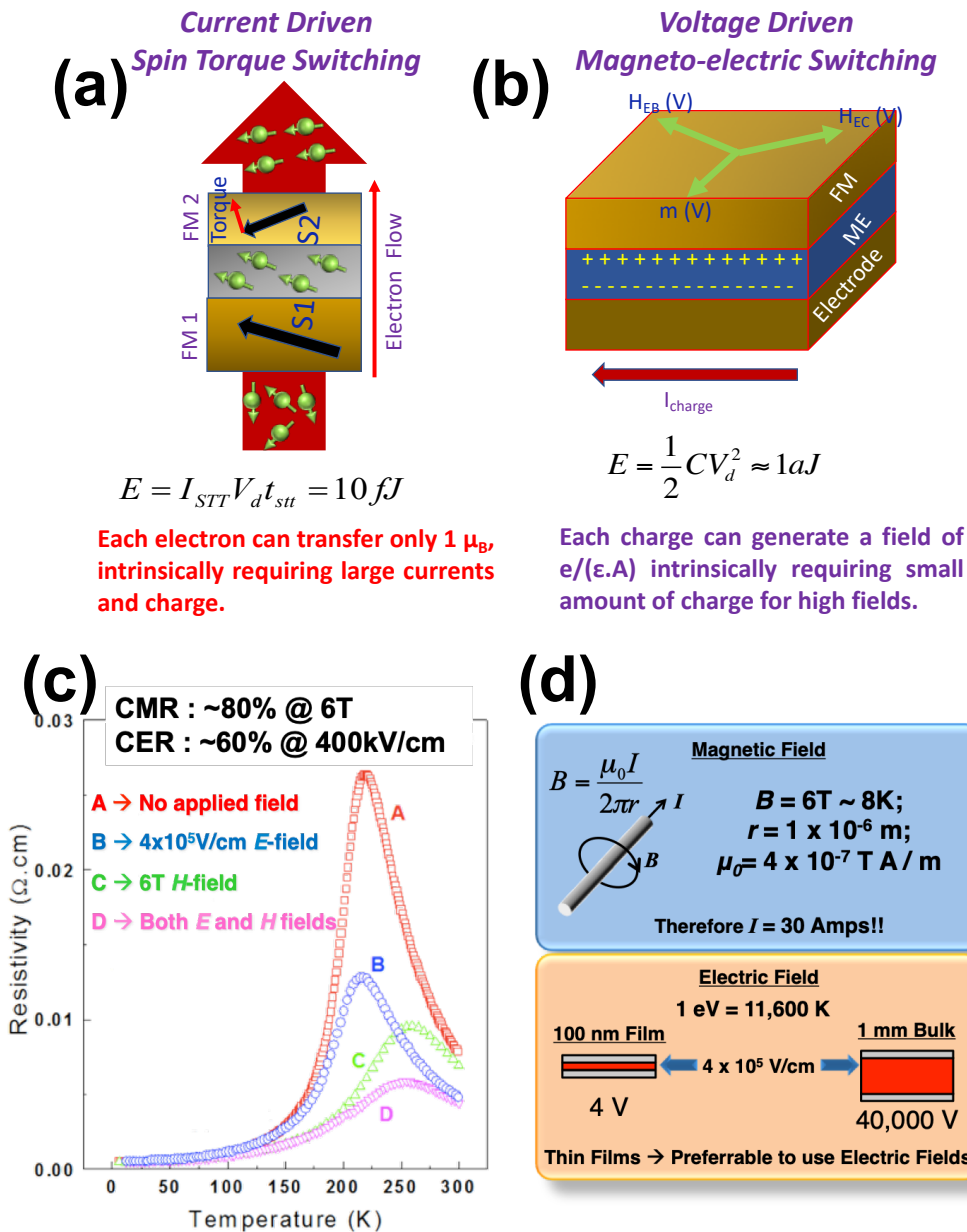


Figure 5: A set of schematics illustrating the energy consumption for nominal devices. (a) On the left is a current driven spin torque switching device and (b) is a voltage driven magnetoelectric switch[18]. (c) presents the original data for the colossal magnetoresistance effect of ~80% at 6T and a ~60% colossal electroresistance effect at an electric field of 400kV/cm; (d) presents a simple calculation of the current required to create a magnetic field of 6T at a distance of 1 micrometer from the center of the current-carrying wire while the bottom shows the calculation of the voltage required to create the 400kV/cm electric field. This voltage scales with the dimensions of the object, while the magnetic field shows not scale with the dimensions of the object. [19]

control magnetism, when it would rather be straightforward to use a magnetic field instead? The answer is energy. In fact, one can potentially reduce the energy consumption by as much as a few orders of magnitude through the use of electric

fields as opposed to magnetic fields. To illustrate this, we explore two possible scenarios. The first describes how a moving electron can create a spin torque, of interest in spin transfer torque (STT) based memory devices. The key is that each electron carries with it a moment of $1 \mu_B$ and therefore generating a large enough spin torque to move domain walls or switch the magnetization requires a large number of electrons (*i.e.*, a large current), which, in turn, requires an appropriate current source (*i.e.*, a battery). For a nominal device dimension (*e.g.*, 10×10 nm lateral dimensions) one can estimate the energy consumed in this process to be on the order of a few fJ (10^{-15} J); (**Fig. 5a**)¹⁸. One can contrast this to a capacitive device, with an electric field modulating the charge, where for a similar 10×10 nm device with a dielectric constant of ~ 100 (which is reasonable for ferroelectrics), one can generate relatively large fields of the order of 10 kV/cm with just about an aJ of energy (10^{-18} J, **Fig. 5b**)! Thus, although this looks like simple physics on the surface, there can be significant impacts for computing when one is either in an Artificial Intelligence (AI)/Machine Learning (ML) or High-Performance Computing (HPC) environment.

We can now look at another interesting aspect of electric and magnetic fields, using the colossal magnetoresistive manganites as an example, Fig.5(c,d)^{19,20}. Fig.5(c) shows the resistivity-temperature plot for the La-Ca-Mn-O system, both as a function of magnetic field (6T), (leading to colossal magnetoresistance) and electric field of 400kV/cm, (leading to colossal electroresistance)²⁰. Fig.5(d) schematically describes an estimate of the current required to generate this magnetic field of 6T at a distance of 1 micrometer from a wire (in the BLUE box, using Ampere's Law), which is of the order of a few Amperes, pointing to a large energy consumption. In contrast, the electric field of 400kV/cm can be generated by an applied voltage of 4V across a 100nm thick film (ORANGE box). The key to note is that the magnetic field does not scale with the size of the object (*i.e.*, the field of 6T is the same, whether the sample is a single macroscopic crystal or a thin film/nanostructure) while the electric potential (which is of greater interest from a practical perspective) scales with the dimensions of the object.

III. Multiferroics and Magnetoelectrics: With this as background, let us now explore the prospects and progress in electric-field control of magnetism with special

attention to multiferroic and magnetoelectric materials. Needless to say, the pace and breadth of the work in this field means that it will be impossible for one manuscript to cover all the developments. Furthermore, this article is also somewhat of a personal perspective of the field; therefore, we direct the reader to a number of excellent recent reviews^{21,22} on this subject for in-depth information on other aspects of such approaches. The manipulation of magnetic properties by an electric field in magnetoelectric multiferroic materials has driven significant research activity with the goal of realizing their transformative technological potential. Here, we review progress in the fundamental understanding and design of new multiferroic materials, advances in characterization and modeling tools to describe them, and explore devices and applications. Focusing on the translation of the many scientific breakthroughs into technological innovations, we identify the key open questions in the field where targeted research activities could have maximum impact in transitioning scientific discoveries into real applications.

III.1 Symmetry and Fundamentals of Magnetoelectric Coupling: Before delving

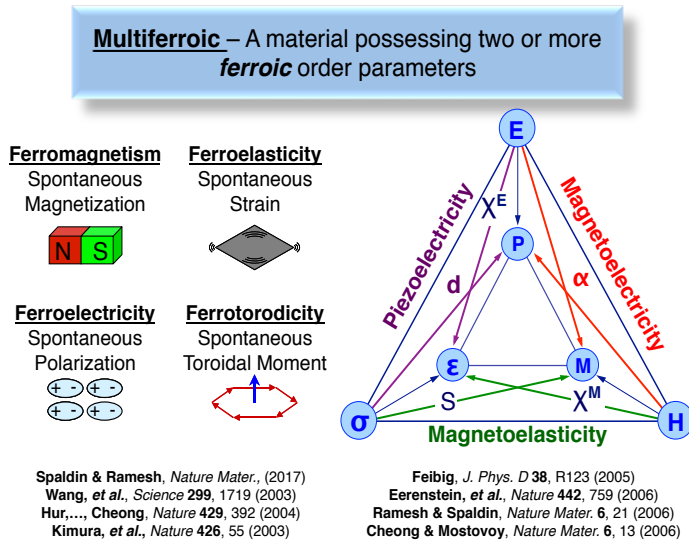


Figure 6: A schematic illustrating the 4 symmetry-based order parameters in solids. On the right is the “Nye-diagram” showing the coupling between the intrinsic and extrinsic thermodynamic variables. [18]

a metal wire wherein the corresponding magnetic field (B) is then given by the right-hand rule, as described in basic physics textbooks. The key symmetry breaking

into specific magnetoelectrics and multiferroics and their applications, it is prudent to describe the symmetry basis for such materials (Fig. 6)¹⁸. Magnetism, for example, breaks time-reversal symmetry. A simple way to visualize this is a classic Amperean experiment in which a current is flowing through

attribute of a magnet is that reversal of the current direction (which is also represented as reversing time), leads to a reversal of the sense of the magnetic field. A ferroelectric, on the other hand, breaks spatial-inversion symmetry (*e.g.*, a mirror plane is lost during the phase transition). In contrast to these two, a ferroelastic (such as martensite) breaks neither time nor spatial inversion symmetry. The apparent lack of a fourth component to complete this picture was recognized in the early years of multiferroics research²³, leading to the addition of a fourth order parameter, namely a ferrotoroidic order (*i.e.*, one which breaks both time and spatial inversion symmetry).

III.2 Multiferroic and Magnetoelectric Materials: Multiferroics exhibit more than one primary ferroic ordering (*i.e.*, ferromagnetism, ferroelectricity, ferroelasticity, or ferrotoroidicity) in the same phase²⁴. This terminology is usually extended to include other types of order such as antiferromagnetism as well as composites of individual ferroics, and is most often used today to refer specifically to magnetoelectric²⁵ materials combining ferroelectric and magnetic behaviors in a single material. Importantly, the combination of ferroic orders in multiferroics can lead to coupling between them, so that one ferroic property can be manipulated with the conjugate field of the other, with particular focus on the prospect of switching the orientation of magnetization using an electric field^{26, 27}. This coexistence and control of simultaneous ferroic order is challenging, requiring design of the electronic structure at the most fundamental level, new materials chemistries to implement them, the development of new tools to compute and characterize the novel properties associated with the coupled behaviors in parallel with new approaches to synthesize such materials with atomic-scale precision. When this is successful, it presents possible routes to entirely new device architectures, as exemplified by the MESO¹⁰ device. This review focuses on the recent developments in these three aspects: basic science, experimental and theoretical methods, and applications of magnetoelectric multiferroics³. We reiterate that the field of multiferroics is now vast, and this article, by its nature reflects, a personal perspective and we thus direct the reader to recent comprehensive reviews with different emphases.^{28,29,30,31,32}

III.3 Pathways to Create Multiferroic and Magnetoelectric Materials. There are now many established routes to circumvent the “contradiction” between ferroelectricity (typically associated with ionic species with empty d -orbitals) and magnetism (typically associated with partially filled d orbitals)³³. Such a “bottoms-up” design is described in the “multiferroic-tree” (**Fig. 7**). A quick perusal of this figure shows that although there are several multiferroics, there is still a dearth of technologically viable multiferroics, *i.e.*, those that can be manipulated at room temperature. Thus, there should be no doubt that a more diverse palette of new materials with robust room-temperature coupling of ferromagnetism and ferroelectricity is still urgently needed and indeed should be the focus of interdisciplinary research. We will return to this later in this section, but first let us delve into currently studied systems. **Table 1** provides a summary of the top five physical principles that have led to the discovery of several multiferroics. Of these,

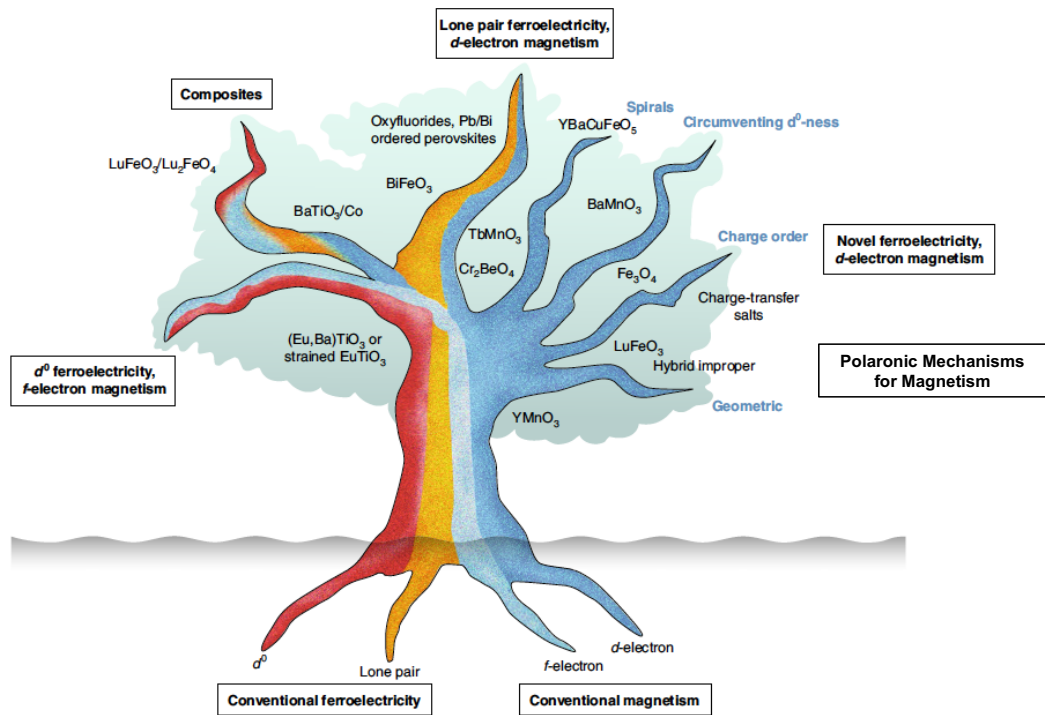


Figure 7: The “Multiferroic Tree” that depicts how one can design multiferroics from the basic elements of bringing together magnetic species (for example, ions with f/d-electrons) and polar species (i.e., chemical species that lead to the emergence of a spontaneous polarization). Each branch depicts exemplar multiferroic systems; the boxes on the outside identify the dominant mechanism responsible for the formation of multiferroics. [22].

the two most studied are multiferroics in which the polar order comes from one of the crystal sites and the magnetic order is built into the other chemical site, as is the case in BiFeO_3 and BiMnO_3 . The second type, which has received considerable interest from the physics community, is based on a polar order emerging as a consequence of a magnetic transition as, for example, in the manganites. An emerging third pathway via the power of heteroepitaxy and superlattice design. We will use these as examples to explore both the fundamental materials physics of coupling as well as the potential for future applications.

III.4 Bismuth ferrite as a model multiferroic: Of the known multiferroics, bismuth ferrite, BiFeO_3 , remains arguably the most important, and certainly the most widely studied, with more than 6000 papers published over the last decade. The

Pathway	Fundamental Mechanism	Example Systems
A-site driven	Stereochemical activity of lone pairs on A-site leads to ferroelectricity; magnetism from B-site	BiFeO₃; BiMnO₃
Geometrically Driven	Long range dipole-dipole interactions and oxygen rotations breaks inversion symmetry	YMnO ₃ ; BaNiF ₄
Charge ordering	Non-centrosymmetric charge ordering leads to ferroelectricity in magnetic materials	LuFe ₂ O ₄
Magnetic Ordering	Ferroelectricity is induced by a lower symmetry ground state that lacks inversion symmetry	TbMnO ₃ ; DyMnO ₃
Atomically Designed Superlattices	Still under investigation; likely lattice mediated	LuFeO₃ – LuFe₂O₄

Table I: This table complements Figure 7. It summarizes the various identified mechanisms for creating multiferroics.

establishment of its large (~90 $\mu\text{C}/\text{cm}^2$) ferroelectric polarization, combined with magnetic ordering persisting well above room temperature³⁴ spawned an intense research effort that continues to unveil fascinating new physics and potential new

applications³⁵. We summarize some of the most compelling recent discoveries here.

BiFeO₃ formally belongs to the perovskite family of oxides, albeit highly rhombohedrally distorted from the cubic prototypical structure. In this phase, the spontaneous polarization points along the eight equivalent $\langle 111 \rangle$ (**Fig. 8**)³⁶. While there was considerable debate as to the magnitude of the spontaneous polarization (which was experimentally measured in epitaxial thin films and predicted theoretically to be $\sim 90 \mu\text{C}/\text{cm}^2$ ³⁷), this value of the spontaneous polarization in the rhombohedral phase is now well established. In parallel with the scientific debate on the ferroelectric properties, there was an equal degree of scientific debate as to the state of magnetism. Magnetism in BiFeO₃ is complex. Although the ground state is a robust G-type antiferromagnetic structure (which can be described by spins in $\{111\}$ that are ferromagnetically coupled in-plane but antiferromagnetically coupled out of plane along the $[111]$), the magnetic structure is quite a bit more sophisticated. Due to antisymmetric Dzyalozhinski-Moriya coupling (which is governed by the crystal symmetry and is allowed for the $R3c$ crystal symmetry of BiFeO₃), a small canted moment arises, which lies in the $\{111\}$ (*i.e.*, perpendicular to the spontaneous polarization direction). Further complication arises in single crystals in which this canted moment spirals about the $[1-10]$ so that it does not exhibit a macroscopically

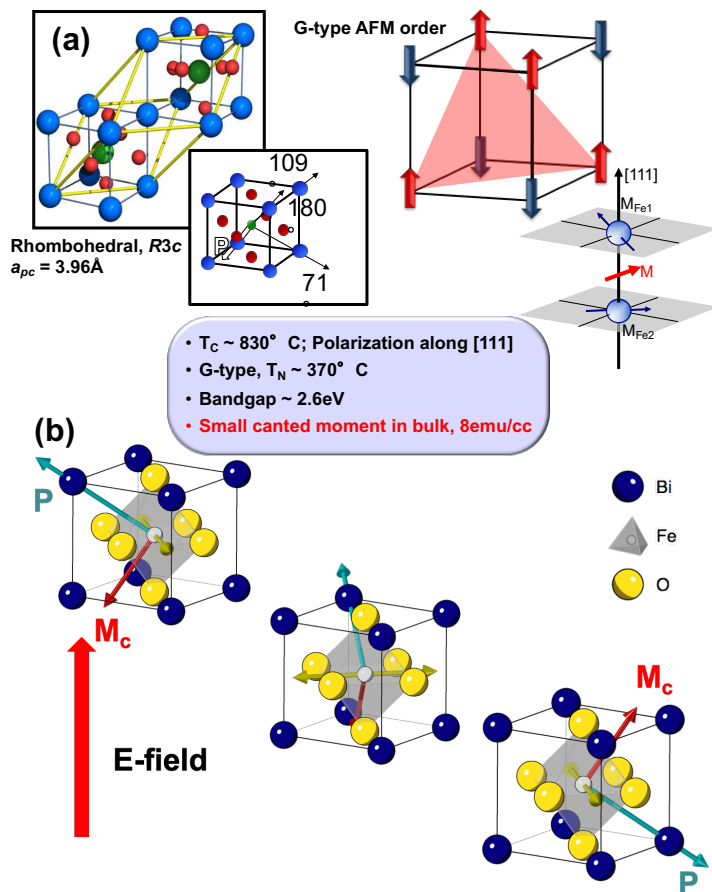


Figure 8: (a) A schematic illustration of the rhombohedral crystal structure of BiFeO₃ as well as the G-type antiferromagnetic order and the canted moment arising as a consequence of the Dzyalozhinski-Moriya coupling; (b) schematically illustrates the 180-degree switching of the polar axis in 2 steps and the associated changes in the canted moment direction.[36].

measurable magnetic moment until this spin spiral is broken, either by elastic strain (for example through epitaxial thin-film growth) or through the application of a magnetic field of ~16-18 T. On top of this, domain walls can play a key role in the emergence of a magnetic moment, which typically manifests in the form of a spin glass. This is discussed in the section on domain walls.

III.5 Chemical Substitutions in Bismuth Ferrite: The role of isovalent and aliovalent chemical substitutions at both the bismuth and iron sites has been extensively studied. Outside of the fundamental understanding of the polar and magnetic order, these studies have also focused on the possibility of creating phase boundaries (much like the morphotropic phase boundary in the $\text{PbZr}_{1-x}\text{Ti}_x\text{O}_3$ family of ferroelectrics) that can lead to large piezoelectric responses and allow for tuning of the ferroelectric switching behavior^{38,39}. Chemical substitutions at the Fe^{3+} site have mainly attempted to manipulate the antiferromagnetic nature (for example

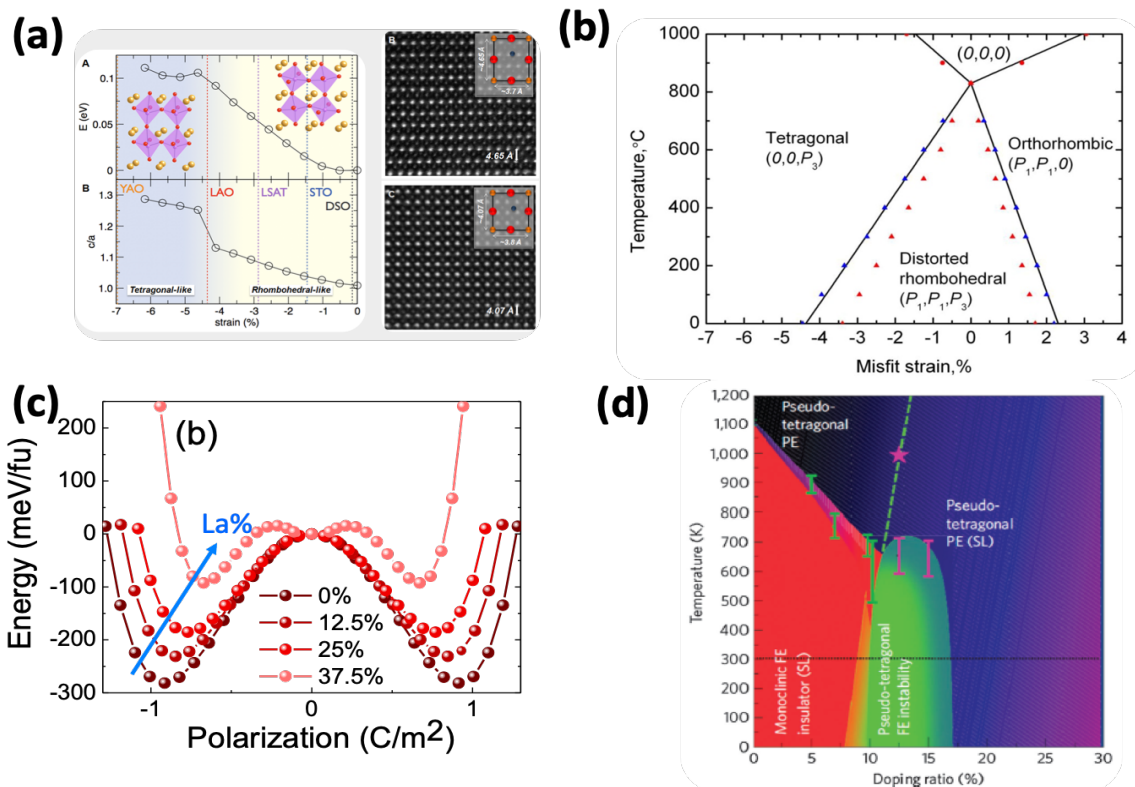


Figure 9: Phase stability in BiFeO_3 . (a) *ab initio* calculation results showing the effects of epitaxial strain on the phase stability[45]; (b) shows phase field results of phase stability[45]; (c) shows the results of *ab initio* calculations on the depth and width of the double well structure for BiFeO_3 as a function of La – substitution [138]; (d) Effect of Ca-substitution on the phase stability in the BiFeO_3 system. [42]

manganese or cobalt substitution has been shown to enhance the magnetic moment)⁴⁰. While these studies have indicated a certain degree of success, detailed studies of the magnetoelectric coupling in such alloyed BiFeO_3 materials are just emerging⁴¹. Indeed, a grand challenge would be to discover pathways to enhance the

magnetic moment to ~ 50 emu/cc (the canted moment in pure BiFeO_3 is only ~ 6 emu/cc) while at the same time demonstrating magnetoelectric coupling (this issue is discussed more in the section on magnetoelectric coupling). Aliovalent substitutions at the Bi-site (for example with Ca^{+2})⁴² destabilizes the polar state and the accompanying oxygen vacancies causes large field dependent conduction and electro-coloration phenomena.

Thin-film synthesis of BiFeO_3 (and other multiferroics) has been a very fruitful pathway to study the materials physics of magnetoelectric coupling as well as pointing the way to possible applications. The perovskite symmetry and lattice parameters (pseudocubic lattice parameter of 3.96 \AA) means that a large number of oxide-based substrates are available for epitaxial synthesis (albeit with varying degrees of lattice mismatch). Thin films with thicknesses down to just a few unit cells and as large as a few microns have been synthesized by physical-vapor deposition (*e.g.*, pulsed laser deposition, sputtering, molecular beam epitaxy), chemical-vapor deposition⁴³, and chemical-solution deposition. Many studies have used conducting perovskite electrodes (such as SrRuO_3 , $\text{La}_{1-x}\text{Sr}_x\text{MnO}_3$, $\text{La}_{1-x}\text{Sr}_x\text{CoO}_3$) as bottom electrodes to both template the perovskite phase as well as provide a bottom contact for electrical measurements. These synthesis studies have led the way to enable a wide range of materials physics studies including thickness-size effects down to just a few unit cells⁴⁴. Consistent with other perovskite ferroelectrics, a suppression of the magnitude of the polar order is observed, although both theory and experiments indicate that a polar state is stable down to even a couple of unit cells.

III.6 Chemical and Elastic Phase Equilibria: Like many ferroelectrics, BiFeO_3 is also quite susceptible to strain. Compressive strains, imposed, for example, through a substrate with a lattice parameter smaller than that of BiFeO_3 (for example SrTiO_3 and LaAlO_3). Under a large ($\sim 5\%$) compressive strain, a super-tetragonal-like (T-like) structure, with an enhanced c/a ratio and an almost square pyramidal iron-oxygen coordination, has been shown to be the stable phase^{45,46,47}. Both *ab initio* theory⁴⁸ and experiments⁴⁹ point to a huge spontaneous polarization of $\sim 150 \mu\text{C}/\text{cm}^2$, oriented

along or close to the [001]. Intriguingly, when BiFeO₃ is grown on LaAlO₃, a mixed phase ensemble of a strained version of the parent rhombohedral (R)-like and super-tetragonal T-like structures is stabilized (**Fig. 9**). This two-phase system has a giant extrinsic piezoelectric response as a consequence of applied electric fields changing the relative fractions of the two phases⁵⁰. In addition, the R-like component has an enhanced magnetic moment that is not yet well understood⁵¹; a microscopic understanding of its magnetism would be valuable in further optimizing the magnetic properties of BiFeO₃. Under biaxial tensile strain, an orthorhombic phase, with ferroelectric polarization in the in-plane [110], has been stabilized by growing BiFeO₃ on orthorhombic NdScO₃ (110) substrates⁵². This structural flexibility of BiFeO₃ reflects the large number of competing low-energy polymorphs^{53,54,55} and points to further exploration of the rich *bulk* crystal chemical phase space in the Bi-Fe-O system⁵⁶. It is likely that several other phases, with different ratios of the parent Bi₂O₃ and Fe₂O₃ oxides are “hidden” within this chemical phase diagram, and could be accessed, for example, by exploiting as-yet unidentified stacking sequences of Fe-O and BiO layers⁵⁷. With on-going improvements in layer-by-layer synthesis techniques, we anticipate the identification of additional phases within this rich phase diagram over the next few years.

III.7 Other Physical Phenomena: In addition to its structural and magnetoelectric richness, large ferroelectric polarization⁵⁸, we mention a number of other intriguing and unexpected behaviors, which are both potentially useful and not yet well understood, that have been observed in nanostructured and nanoparticulate BiFeO₃. These include a photovoltaic effect ⁵⁹ , photocatalysis ⁶⁰ , photostriction ⁶¹ , electrochromism^{62,63}, and gas-sensing behavior⁶⁴. While not directly exploiting the multiferroic properties of BiFeO₃, it is likely that the presence of the magnetic iron 3*d* states in the region of the band gap, which change both the magnitude of the band gap and the symmetry of the band edges, combined with the internal electric fields from the ferroelectric polarization, are relevant. Research on these aspects of BiFeO₃ will undoubtedly expand over the coming years. Particularly important will be an improved understanding of the properties of BiFeO₃ surfaces, where a surface skin

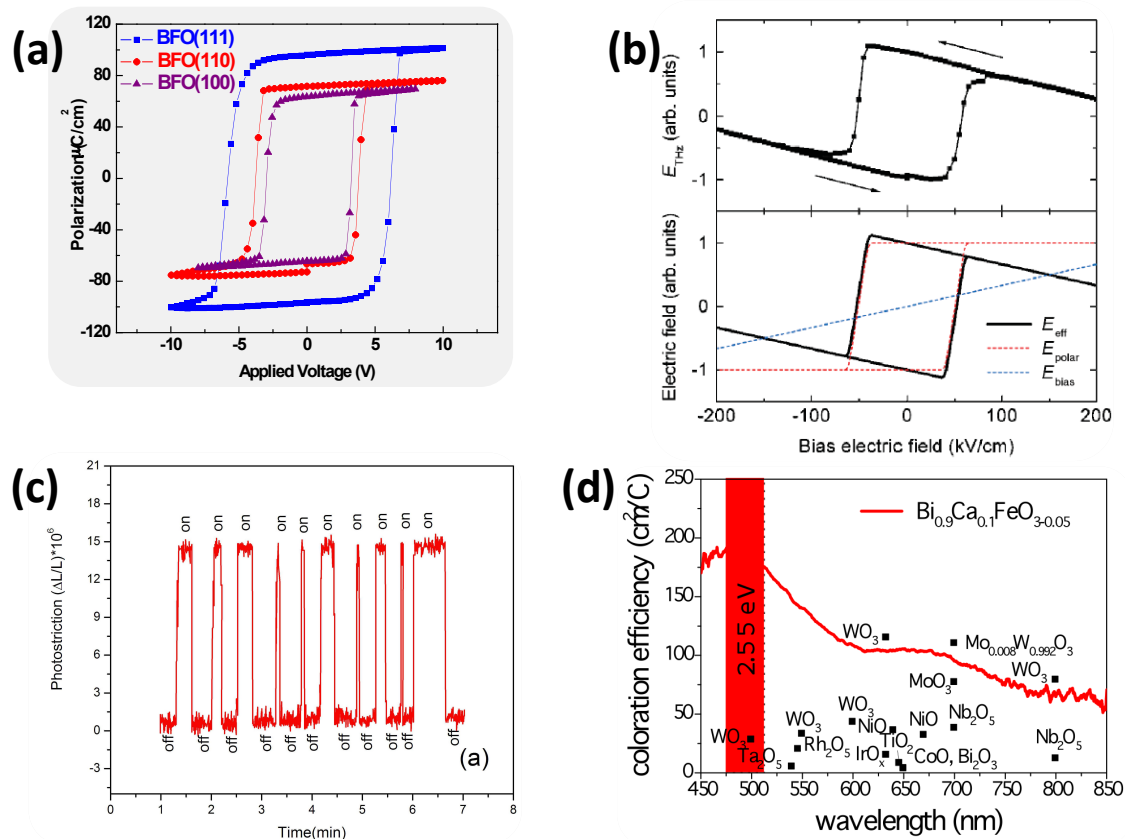


Figure 10: (a) polarization-voltage hysteresis loops for various orientations of the model multiferroic, BiFeO₃ [58]; (b) Thz response loops for BiFeO₃; [73] (c) large photostriction in BiFeO₃ crystals; [61]; (d) large photochromic effects in Ca-BiFeO₃. [63]

layer with different structure and properties from the bulk has been reported^{65,66}, as well as further studies of the effect of size on nanoparticle properties⁶⁷.

The emergence of a host of novel probes, including those based on electrons, ions, photons, and neutrons as well as proximal probes has enabled the discovery of several of the above-mentioned physical phenomena. While it is not the intention of this review to go into each of them in detail, a short summary is presented to put them into context. The past years have seen the development and implementation of a variety of new experimental tools that offer the promise of studying the spin, charge, and orbital degrees of freedom in multiferroics, with a spatial resolution approaching the unit-cell dimensions, and with sub-femtosecond time resolution.⁶⁸ Such local and time-resolved characterization of the magnetoelectric coupling is already leading to the identification of new physics that could not be revealed by the spatial or temporal ensemble-averaged bulk measurements used to date⁶⁹. Scanning-probe techniques, such as piezoresponse force microscopy (PFM), conducting-atomic force microscopy (c-AFM), and magnetic force microscopy (MFM) are particularly attractive since they combine spatial resolution and functional response. We direct the reader to recent reviews for an in-depth treatment of these techniques⁷⁰, mentioning here specifically the recent use of tips containing diamond nitrogen-vacancy (NV) centers to probe the spiral magnetic moment in BiFeO₃⁷¹. In the same vein, time-resolved X-ray studies can now reveal the dynamics of coupling between spin and charge degrees of freedom, with ultrafast synchrotron X-ray sources⁷² complementing table-top femtosecond laser-based probes. In one example, terahertz (THz) radiation arising from multiferroic BiFeO₃ thin films during ultrafast modulation of the spontaneous polarization was probed with femtosecond laser pulses and shown to directly reflect the polarization state, suggesting the possibility of using this as a memory read-out mechanism⁷³.

Electron probes can now reveal chemical information, through electron energy loss spectroscopy (EELS), and structural information, using aberration-corrected microscopes, at sub-Å spatial resolution. Light elements such as oxygen, and their octahedral rotations and tilts in perovskites, can be identified⁷⁴. These are of particular importance since they determine bandwidths and magnetic exchange, to

which the magnetic and ferroelectric properties are sensitive. In addition, magnetic information can now be extracted from electron circular dichroism measurements, in which zone plates induce helicity in the electron beam⁷⁵. Optical second-harmonic generation is a well-established tool for probing ferroelectricity due to its sensitivity to inversion-symmetry breaking⁷⁶. The recent implementation of *in situ* second harmonic generation during pulsed laser deposition oxide growth is particularly promising for understanding the emergence of ferroelectric order in materials such as BiFeO₃, in which the growth occurs below the ferroelectric Curie temperature⁷⁷.

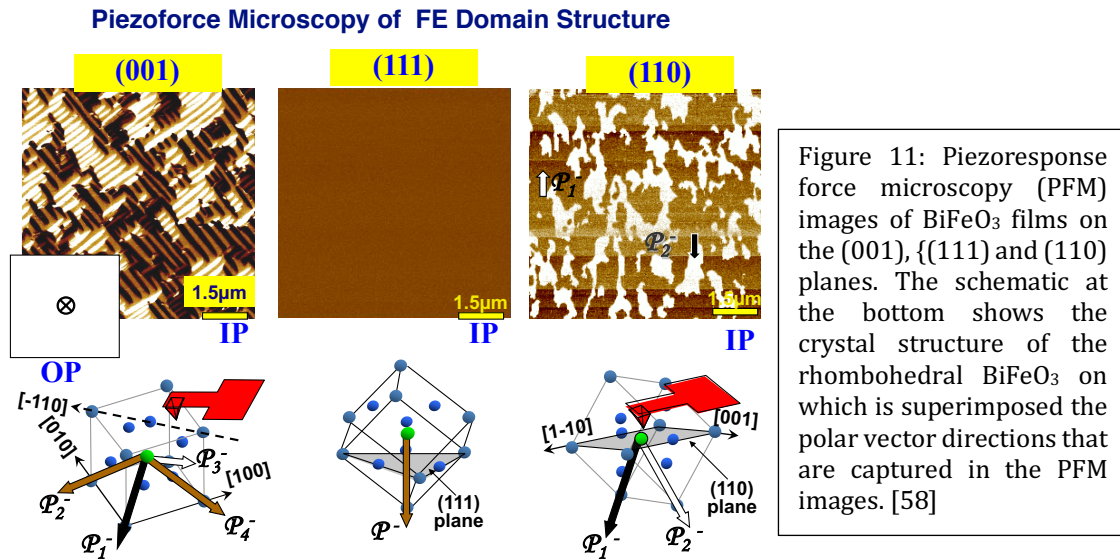
III.8 Theoretical Studies: While first-principles density functional theory (DFT) calculations remain the gold standard for understanding and predicting the properties of ferroelectrics and multiferroics, second-principles calculations are proving increasingly valuable in the study of larger scale systems, for example heterostructures, domain walls and defects, as well as longer timescales in molecular dynamics⁷⁸. In second-principles calculations, an effective model is constructed by a judicious choice of the essential physics, and the parameters of the model are extracted by fitting to DFT. Such effective models have been used successfully applied for many years to describe structural phase transitions of prototypical ferroelectrics^{79,80}, and recent extensions to include additional lattice degrees of freedom⁸¹, as well as magnetic interactions⁸², have extended their applicability to multiferroics. For example, an effective Hamiltonian consisting of a lattice part incorporating ferroelectric distortions, octahedral rotations and strain, a contribution from the interaction of the magnetic moments with each other, and coupling between the magnetic moments and the lattice, has been shown to accurately reproduce the crystal and magnetic structures of bulk BiFeO₃. One length scale further, a Landau-Ginzburg thermodynamic potential that includes both polar and antiferrodistortive distortions and their coupling to the magnetism has been successful in reproducing the bulk behavior of BiFeO₃ and offers great promise for predicting properties in thin film heterostructures and nanostructures.⁸³

Going forward, improved multi-scale approaches that allow treatment of the electronic and lattice degrees of freedom on the same footing⁸⁴ could lead to vastly

enhanced system size and accuracy when combined with improved tools for generating effective potentials using input from first principles⁸⁵. Modeling of the dynamics of ferroelectric switching⁸⁶ and its effect on magnetic order⁸⁷, both of which are on time- and length-scales that are far outside the ranges accessible using density functional methods, now become feasible. Such models in combination with molecular dynamics start to allow calculation of dynamical magnetoelectric responses in the THz region⁸⁸, which is particularly timely as it coincides with advances in experimental methods for generating THz radiation mentioned above. Finally, the ongoing development of new theoretical concepts, such as the magnetoelectric multipole as an order parameter for phase transitions that break both space-inversion and time-reversal^{89 90}, as well as the production of practical computational tools for their calculation look very promising in terms of pushing the limits of computationally driven materials discovery.^{91,92,93,94}

III.9 Domains and Domain Walls in Multiferroics: As in other ferroelectrics, domains form as a result of electrostatic and elastic energy minimization and the change in the polarization vector direction upon moving from one domain to another identifies the nature of the domain wall that separates two domains. In the case of BiFeO₃, the rhombohedral symmetry leads to domains that reflect this and hence we observe 71°, 109°, and 180° domain walls. The 71° and 109° walls are also ferroelastic in nature and thus exist to accommodate elastic energy arising, for example, due to lattice mismatch with the substrate. In the case of thin films formed on substrates of various orientations, this is reflected in the domain patterns that emerge. Typical manifestations of these domain walls in piezoresponse force microscopy (**Fig. 11a-c**) and schematically (**Fig. 11d-f**) reveal the range of domain structures possible in epitaxial thin films of BiFeO₃.

The remarkable observation of electrical conductivity at certain ferroelectric domain walls in BiFeO_3 ^{95,96} opened an entirely new avenue of research into novel functionalities at multiferroic domain walls (**Fig. 12a**) which was motivated by the prospect of metallic transport through nanoscale channels that can be electrically written, erased, and moved.^{97, 98} The emergence of transport in an otherwise insulating material is, by itself, a fascinating materials physics question. Temperature and magnetic field dependent studies show large magnetoresistance and increasing conductivity as temperature is decreased below $\sim 50 \text{ K}$ ⁹⁹, suggesting the possibility of metallic transport at the domain walls; such a demonstration in an otherwise insulating ferroelectric would be a significant breakthrough. Subsequent studies have



revealed a wealth of behavior ranging from large memristive behavior (**Fig. 12b**), magnetoresistance^{100, 101}, spin transport^{99, 102} (**Fig. 12c**), and photovoltaic response¹⁰³. In addition, conducting ferroelectric domain walls have been identified in several other materials, including improper ferroelectrics such as ErMnO_3 ¹⁰⁴ (**Fig. 13**). There, head-to-head and tail-to-tail domain walls are trapped by the topology of the domains caused by the improper ferroelectric phase transition, and the low spontaneous polarization facilitates compensation of the associated polar discontinuity by changes in the electronic band structure. Intriguingly, the prototypical non-magnetic ferroelectric, BaTiO_3 , has recently been manipulated to

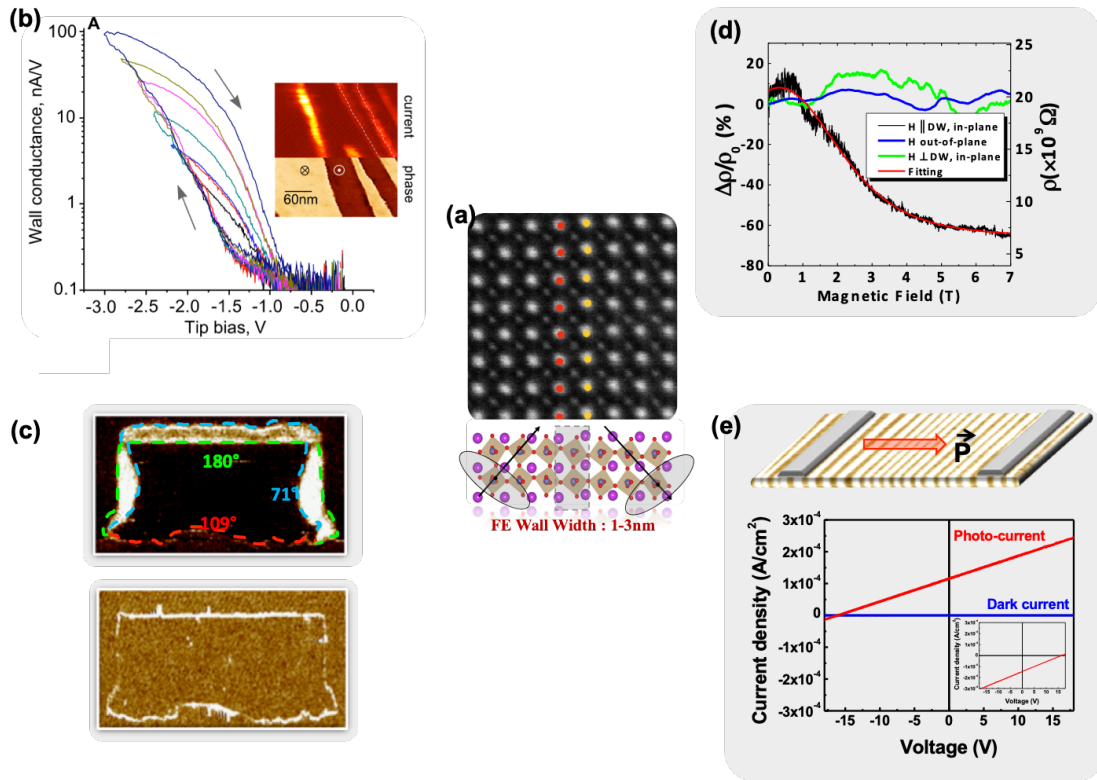


Figure 12: (a) an atomic resolution image of a 109° domain wall in BiFeO_3 ; [26] (b) UHV conducting -AFM measurement of voltage dependent transport at a 109° domain wall [101]; (c) PFM (top) and conducting AFM (bottom) image of domain patterns illustrating current transport at 109° and 180° domain walls [95]; (d) normalized change in the resistivity as a function of magnetic field for fields parallel and perpendicular to the 109° domain wall arrays. [99]; (e) photovoltaic responses from an array of 71° domain walls in BiFeO_3 showing a large open circuit photovoltage as a consequence of voltage drops across the domain walls [103].

accommodate charged domain walls which are also conducting¹⁰⁵. A two-dimensional, ferromagnetic phase has also been observed at the twin-domain walls of antiferromagnetic TbMnO_3 .^{106,107} Future progress on domain-wall functionality will rely on detailed calculations and careful characterization to clarify the origin of the observed behavior¹⁰⁸. Important open questions are: (i) can we create configurational changes at a domain wall leading to different physical properties? (ii) what are the limits of possible electron transport; (iii) can a metal-to-insulator transition be achieved and controlled. In a similar vein, the potential for memristive behavior and the role of proper versus improper ferroelectricity in determining the domain wall properties and switching dynamics would be valuable to explore. A

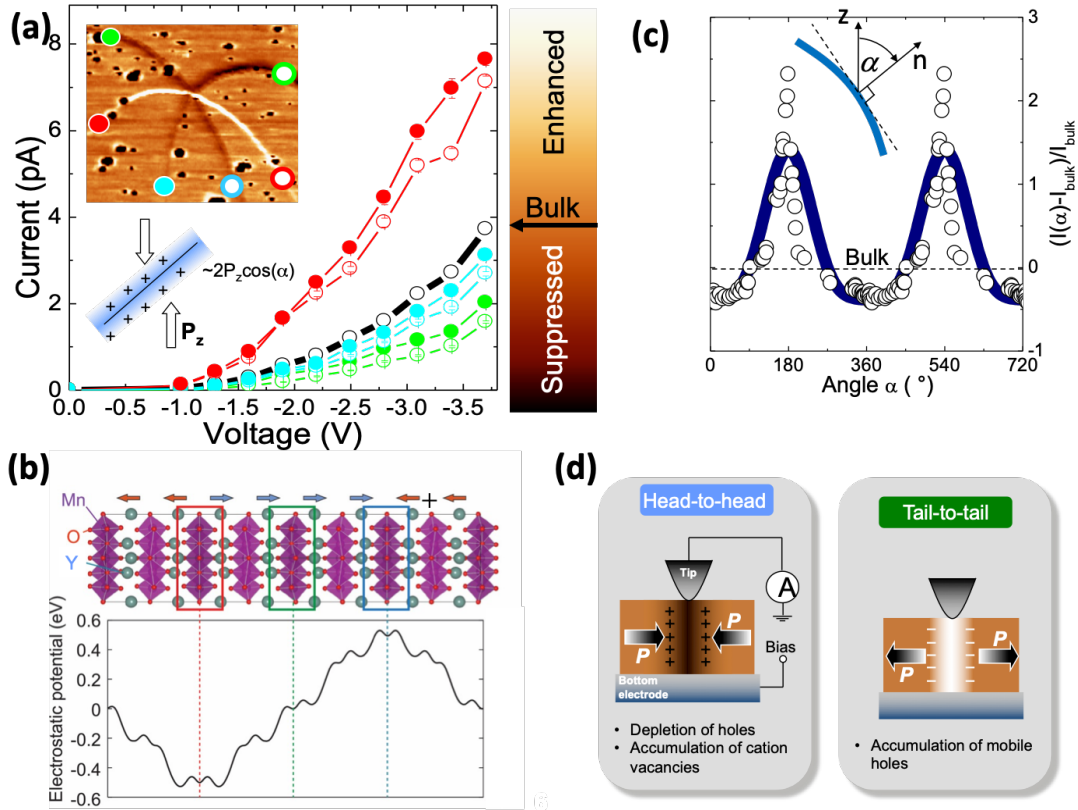


Figure 13: (a) shows current-voltage plots at various locations on head-to-head and tail-to-tail domain walls, which are captured in the conducting AFM image in the inset; the schematic below shows the angle dependence of the polarization across the wall (which influences the band bending at the wall)[104]; (b) shows a schematic of the domain wall and a calculated plot of the electrostatic potential across the wall; (c) normalized, angle-dependent current through the domain walls; (d) A schematic illustration of the depletion of holes (at head-to-head walls) and enhancement of holes (at tail-to-tail walls) and how the conducting AFM senses these changes. [104].

comprehensive review of domain-wall physics and possible applications has been recently published¹⁰⁹.

IV Magnetolectric Coupling

IV.1 Magnetolectric Coupling and Heterostructures: Armed with some basic understanding of the order parameters and symmetry in systems such as BiFeO_3 , we can now ask perhaps the most important question: how does magnetism couple to an electric field such that the state and direction of magnetism can be manipulated through the application of an electric field? In nature this coupling between electricity and magnetism occurs through electromagnetism. However, in order to be able to

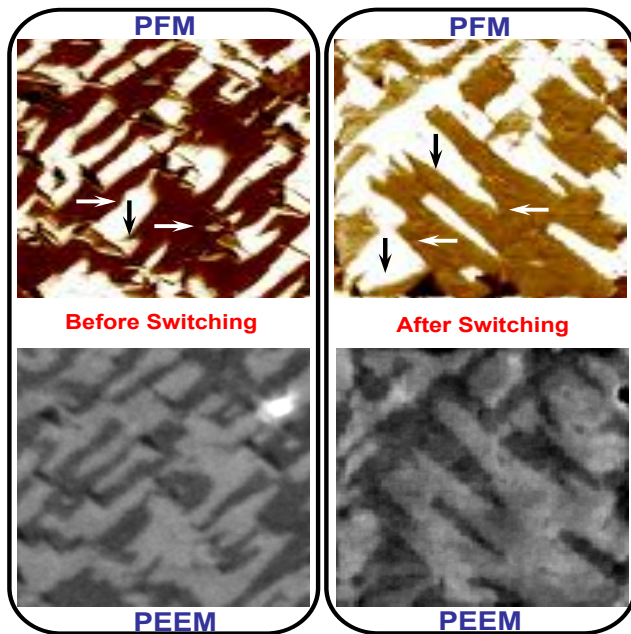


Figure 14: electric field control of antiferromagnetism probed using XLD-PEEM. On the left is piezoforce microscopy showing the ferroelectric domain structure before switching; the corresponding XLD-PEEM image (probing antiferromagnetism) is shown at the left bottom. The corresponding PFM/PEEM images after switching are shown to the right. [118].

dramatically change the state of magnetism with an electric field, it is desirable for the magnetoelectric coupling to be significantly stronger than what is available in nature.

In turn, such coupling makes possible a range of microelectronic device applications which make use of judicious heterostructure design. We point the reader to other reviews describing the permeation of multiferroics into other scientific fields^{110,111}. The driver for studying electric-field control of magnetism, as noted above, is the substantially lower energy requirement for manipulating magnetic states with electric rather than magnetic fields. As we described (**Fig. 5**), in the state-of-the-art spin transfer torque approach to reorienting magnetism, each electron's $1 \mu_B$ of spin switches $1 \mu_B$ of magnetization. The required current increases linearly with the size of the moment to be switched, amounting to a current density of $\sim 10^{11} \text{A/m}^2$ and an energy consumption of $\sim 10 \text{ fJ}$ in a typical $10 \text{ nm} \times 10 \text{ nm}$ device. For comparison, the total energy consumed in the capacitive multiferroic device described below, for the same $10 \text{ nm} \times 10 \text{ nm}$ lateral geometry, is just $\sim 1 \text{ aJ}$, four orders of magnitude smaller^{112,113}. In this section, we review recent advances in two aspects of electric-field control of magnetization^{114,115,116}.

Among the handful of multiferroics, BiFeO_3 is one of the most studied systems for a few important reasons: (i) It is perhaps one of the earliest identified “correlated

electron” systems (similar to the manganites and more recently the iridates) wherein, without introducing electron-electron correlations, the material is essentially a weak semiconductor with a small bandgap¹¹⁷ but with correlations undergoes the opening up of a gap of ~ 2.7 eV and thus exhibits insulating behavior. (ii) It has robust magnetic and ferroelectric ordering at room temperature. Finally, and perhaps most importantly, (iii) although it does not show a linear magnetoelectric coupling in the bulk due to the existence of the aforementioned spin spiral, it does show linear magnetoelectric coupling in thin films, since the spiral is typically broken.

Understanding the potential for electric-field control of antiferromagnetism requires probing the magnetism using X-rays or neutrons since direct magnetometry studies are not effective for antiferromagnets. Such studies of BiFeO₃ have shown that when the polarization state switches with the application of an electric field, there is a corresponding rotation of the magnetic order^{118,119}. Such a change can also be spatially probed using a combination of piezoresponse force microscopy to image the ferroelectric order and X-ray magnetic linear dichroism (XLD) photoemission electron microscopy (PEEM) to image the antiferromagnetic order, (**Fig. 14**). It is interesting to note that there has been little detailed work on a full understanding of how the antiferromagnetic state is manipulated by an electric field – with most studies assuming the magnetic order merely follows that of the polar order, but not clarifying that pathway. This is particularly surprising, since the antiferromagnetic resonance frequencies are in the several hundred GHz range and BiFeO₃ has ferromagnons in the 700 GHz to 1 THz range. Given the current surge in interest in antiferromagnetic spintronics, we expect that such insulating multiferroics which exhibit electrical field controllable antiferromagnetism would also garner more interest, specifically from the high frequency community.

This said, multiferroic coupling has been shown even in the mixed-phase versions of BiFeO₃ described above. By way of a brief recap, recall that when one grows BiFeO₃ on LaAlO₃ substrates (with a nearly 5% compressive strain from the parent rhombohedral phase), a super-tetragonal-like (T-like) structure is created which coexists with a strained phase derived from the parent rhombohedral (R)-like phase (**Fig. 15a,b**). This two-phase system has a giant extrinsic piezoelectric response

as a consequence of applied electric fields changing the relative fractions of the two phases¹²⁰. Using X-ray magnetic circular dichroism-based photoemission electron microscopy coupled with macroscopic magnetic measurements, it was found that the spontaneous magnetization of the rhombohedral-like phase in these mixed-phase

samples is significantly enhanced above the canted antiferromagnetic moment in the bulk phase, as a consequence of a piezomagnetic coupling to the adjacent tetragonal-like phase and the epitaxial constraint (**Fig. 15c**)¹²¹. Subsequently, reversible electric-field control and manipulation of this magnetic moment at room temperature was

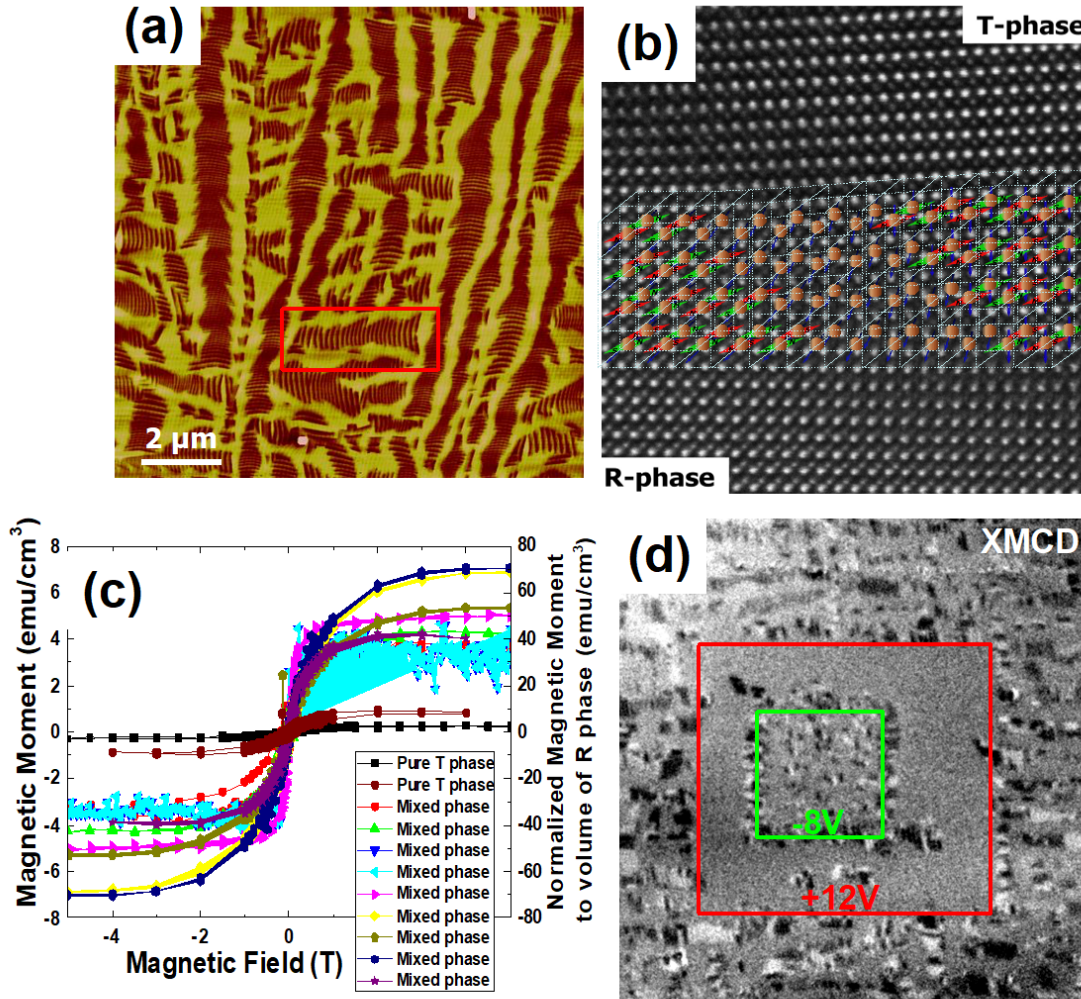


Figure 15: (a) and AFM topography image showing the formation of a nanoscale mixed phase ensemble in a epitaxial BiFeO₃ film grown under highly compressive conditions (on a LaAlO₃ substrate); the dark stripes are regions of a highly distorted rhombohedral phase that is epitaxially constrained within a matrix of the super-tetragonal phase; (b) A high resolution image of the interface between the Rhombohedral (R-phase) and tetragonal phase (T-phase) showing the progressive rotation of the spins from one phase to the other; (c) experimentally measured magnetic moment of samples with varying fractions of the mixed R/T-phases compared to the pure T-phase; the right y-axis shows the magnetic moment that is normalized to the volume fraction of the R-phase, showing the strong enhancement of the moment in the R-phase due to the constraint imposed by the T-phase around it; (d) is an XMCD-PEEM image obtained at the Fe absorption edge, as a function of electric field applied to local regions; Strong magnetic contrast is observed in the regions corresponding to the strained R-phase; with a +12V, the entire region is converted to the T-phase; upon switching back with a -8V pulse, the system returns to the mixed R/T-phase which is manifested in the appearance of magnetic contrast in the inner box. [121]

also shown (Fig. 15d). All of this points to the great potential of BiFeO₃-based systems for potential multiferroic/magnetoelectric applications.

IV.2 Electric field control of mixed magnetic states and nanocomposites.

Early on in the evolution of the modern version of multiferroics and magnetolectrics¹²², it was realized that nanocomposites comprised of ferrimagnets embedded (in many cases epitaxially) in a ferroelectric/piezoelectric matrix could lead to efficient magnetolectric coupling controlled by interfacial epitaxy. Such nanocomposites, exemplified by single crystalline nanopillars (Fig. 16a) of ferrimagnetic spinels (*e.g.*, CoFe₂O₄) embedded epitaxially in a ferroelectric perovskite matrix (*e.g.*, BiFeO₃), are illustrated in the AFM images (Fig. 16b). The

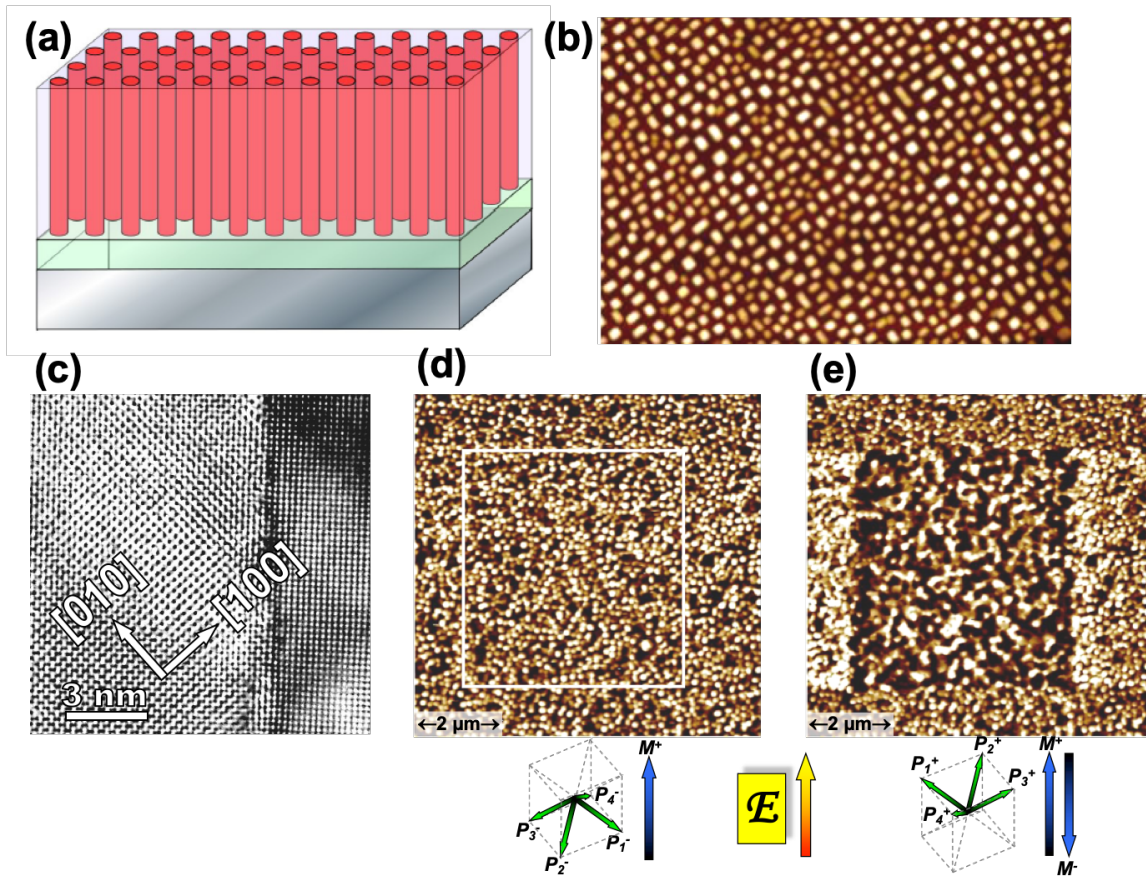


Figure 16: (a) a schematic of the 3-D vertically epitaxial magnetolectric nanocomposite [122]; (b) AFM image of the ferrimagnetic CoFe₂O₄ nanopillars (in bright contrast embedded in a ferroelectric BiFeO₃ matrix (in dark contrast); (c) A high resolution STEM image of the interface between the spinel ferrimagnet and the perovskite ferroelectric ; (d) is a magnetic force microscopy (MFM) image after magnetization at 2T, in which the ferrimagnetic nanopillars appear in bright contrast; (e) is the corresponding MFM image after the matrix was switched with a -16V applied with an AFM tip. The schematics below describe the magnetic state before and after the electric field switching [123].

epitaxial nature of the lateral interfaces is shown in corresponding planar section TEM images (**Fig. 16c**). Electric field driven switching studies of such nanocomposites reveals perhaps the most interesting aspects of such nanocomposites of relevance to deterministic switching of the magnetic state with an electric field: that, while the initially magnetized state (**Fig. 16d**), can be switched with an electric field, only ~50% of the magnetic nanopillars switch their state (for example from magnetization pointing up to down; **Figs. 16d,e**). Detailed analysis of this data¹²³ revealed that this is indeed true and arises from the fact that the electric field assists in manipulating the magnetic anisotropy of the ferrimagnetic nanopillar. However, the magnetic anisotropy of the nanopillar is the same whether it is magnetized up or down (along the long axis of the nanopillars), thus leading to an ~50/50 mixture of up/down states after the electric field manipulation. This study also throws light on the most important physics of such coupling phenomena, namely that manipulating the magnetization direction in a deterministic fashion, for example by 180°, requires that there be a field that breaks time-reversal symmetry. Said another way – the electric field and corresponding piezoelectric stress that is generated does not break time-reversal symmetry and thus cannot deterministically switch the magnetization. But application of a small magnetic field to the nanopillar arrays during the electric field induced switching event leads to a complete switching of their magnetic state. These

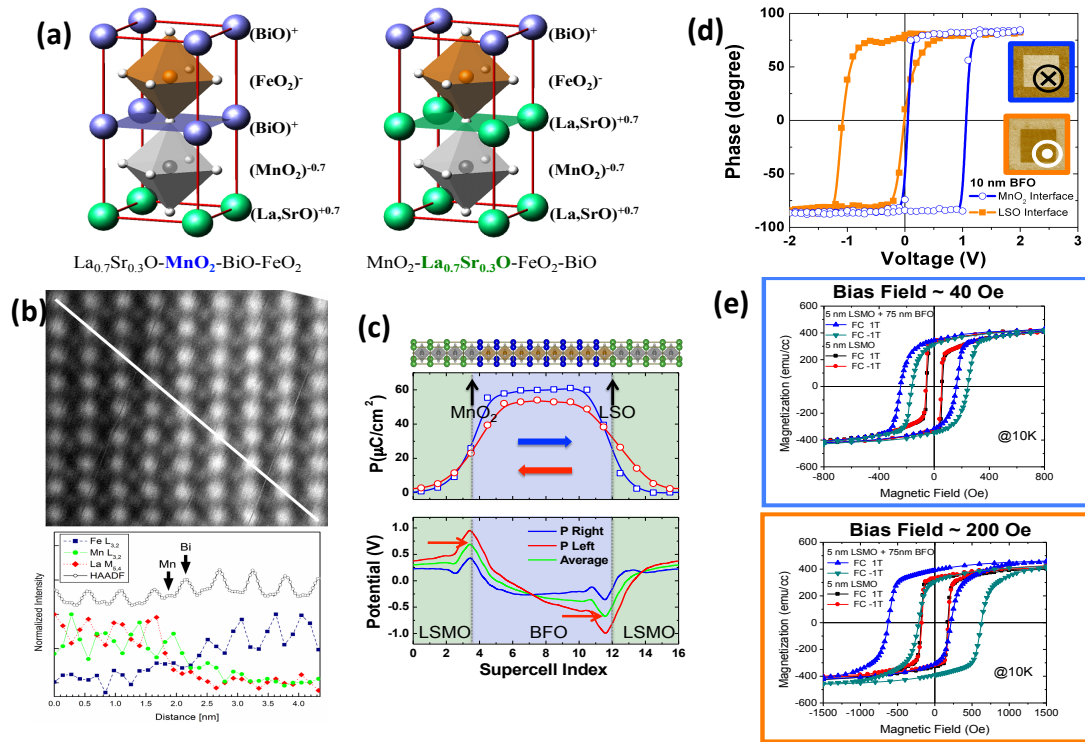


Figure 17: (a) crystal structure model of the LSMO/BFO interface for the Bi-O and (La,Sr)-O interface termination; (b) is an atomic resolution image of the LSMO-BFO interface with the corresponding EELS scan across this interface ; (c) is a calculated plot of the polarization and the interface potential for the two types of interfaces ; (d) piezoforce microscopy (PFM) phase angle as a function of voltage for the two types of interfaces, showing the build-up of an interface potential due to the termination [126] ; (e) depicts how the exchange coupling at the interface changes with the termination (measured at 10K) [127].

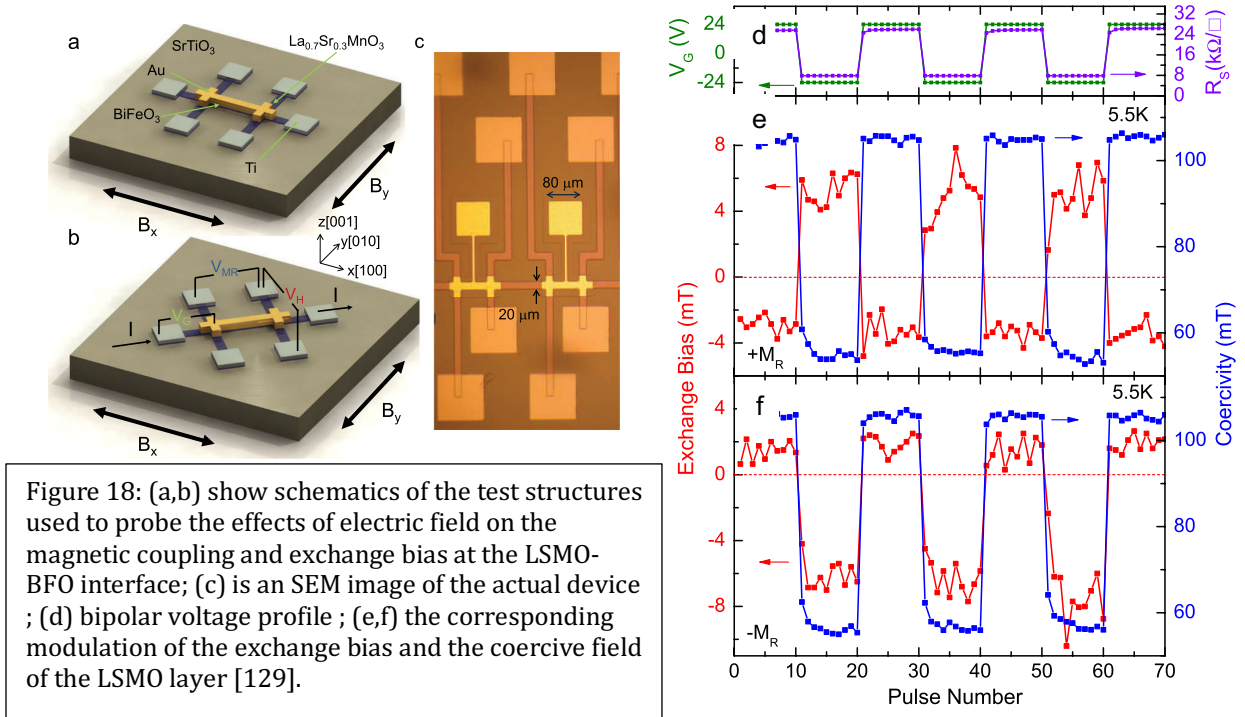
results also point to the need to have a coupling mechanism that is magnetic in nature, for example, interfacial exchange bias coupling, which we focus on next.

IV.3 Electric-field control of magnetic orientation through interfacial exchange coupling. Perhaps the most significant breakthrough in the last years is the demonstration that the magnetization in conventional ferromagnets (*e.g.*, Co_{1-x}Fe_x) can be rotated by 180° by an electric field^{124,125} when it is exchange coupled to BiFeO₃. The extension to all-oxide La_{0.7}Sr_{0.3}MnO₃/BiFeO₃ interfaces (**Fig. 17**), with chemically abrupt A-site termination^{126, 127}, allowed for electric-field control of exchange bias coupling, albeit at temperatures below 100 K^{128,129}.

Despite this limitation, researchers were able to achieve electric-field control of the exchange bias in such heterostructures. While attempts at electric-field control of exchange bias had been made before, it has been shown to be difficult to achieve

full control. Earlier work on the same system has shown the ability to reversibly switch between two exchange bias states with the same polarity (unipolar modulation) without the need for additional magnetic or electric fields in a multiferroic field effect device, but eventually researchers demonstrated the ability to reversibly switch between two exchange bias states with opposite polarity (bipolar modulation) as well (**Fig. 18**). The key was modifying the direction of the magnetization in the $\text{La}_{0.7}\text{Sr}_{0.3}\text{MnO}_3$ with respect to the current in the device channel. A reversible shift of the polarity of exchange bias through the zero applied magnetic field axis was thus achieved with no magnetic or electric-field cooling, no temperature cycling, and no additional electric or magnetic bias fields – in essence, full direct electric field control of exchange bias. This structure also further helped clarify the mechanism underlying the change in exchange bias coupling.

With all this said and despite the exciting advances, an important open problem is the development of oxide ferro- or ferri- magnets with high T_c , a significant remanent moment and strong exchange coupling and Ohmic contacts with BiFeO_3 or another multiferroic. Spinel or double perovskites are promising candidates in this regard. In a complementary direction, the antiferromagnetic domain orientation in



magnetoelectric Cr_2O_3 , which can be controlled by an electric field, has been shown to affect the exchange-bias coupling to a ferromagnetic overlayer¹³⁰ opening a pathway to electric-field switchable exchange-bias devices.

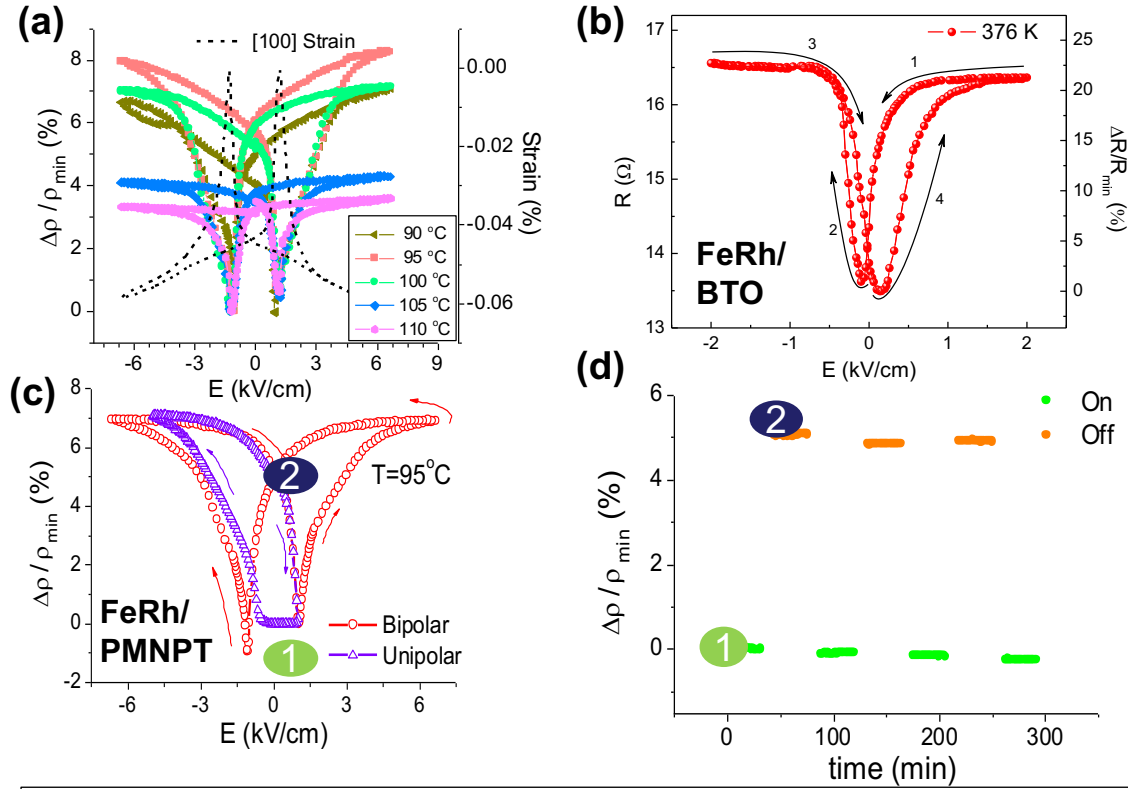


Figure 19: (a) normalized resistivity change in the $\text{Fe}_{1-x}\text{Rh}_x$ layer as a function of electric field applied to the PMN-PT substrate; the corresponding strain in the PMN-PT layer is shown in dotted lines; (b) another example of the modulation of the $\text{Fe}_{1-x}\text{Rh}_x$ resistivity using a BaTiO_3 single crystal; (c) an example of the normalized change in the resistivity of the Fe-Rh layer showing the existence of two nonvolatile states that are captured in the time-dependent measurements in (d) [134,135].

IV.4 Electric-field control of magnetic state: In parallel to these efforts to control the orientation of magnetization with an electric field using multiferroics such as BiFeO_3 , there have been successes in electric-field manipulation of the magnetic state, for example, in changing between ferromagnetism and antiferromagnetism using composite systems as well. One example is electric-field modification of the magnetic exchange interactions in magnetic $\text{Fe}_{1-x}\text{Rh}_x$ heterostructured with piezoelectric $(1-x)\text{Pb}(\text{Mg}_{1/3}\text{Nb}_{2/3})\text{O}_3-x\text{PbTiO}_3$ (PMN-PT). Motivated by the long-known volume collapse at the ferromagnetic to antiferromagnetic transition in $\text{Fe}_{1-x}\text{Rh}_x$ ^{131,132}, an electric field was used to drive the reciprocal effect, a ferromagnet-to-

antiferromagnet transition induced by a structural deformation^{133,134,135} (**Fig. 19**). Since the resistivities of the two magnetic phases differ, the magnetic transition is accompanied by a $\sim 25\%$ change in film resistivity. Open challenges include reducing the optimal working temperature from around 100°C to room temperature, tuning the chemical composition to optimize the strengths of the exchange interactions, achieving complete conversion between the ferromagnetic and antiferromagnetic phases and reducing the required applied voltages. Other promising systems are the Mn-Pt intermetallics and half-doped perovskite manganites such as $\text{La}_{0.5}\text{Sr}_{0.5}\text{MnO}_3$, in which an electric-field-driven charge-ordered antiferromagnetic insulator to ferromagnetic metal transition could be possible.

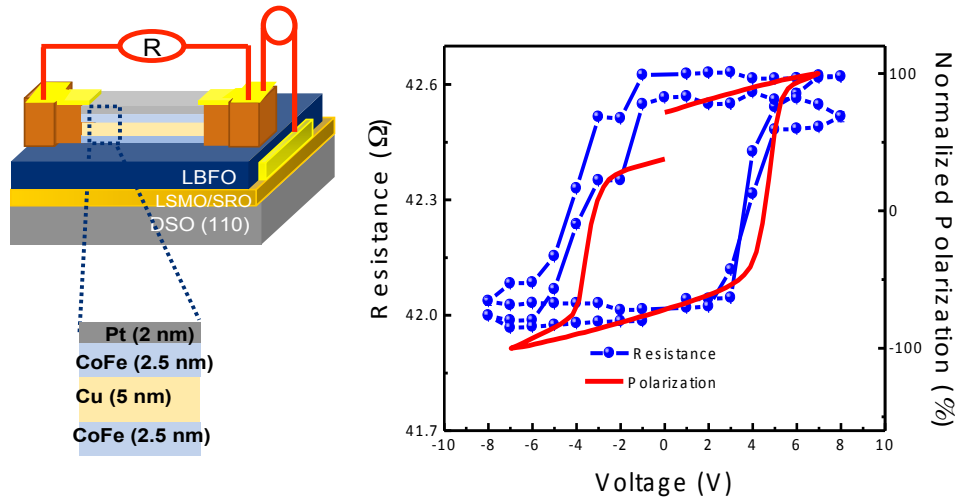


Figure 20: (a) a schematic of the test structure used to probe the electric field dependent manipulation of the magnetic state in a CoFe-Cu-CoFe spin valve; (b) the corresponding voltage dependent magnetoresistance of the spin valve (BLUE), superimposed on the ferroelectric polarization-voltage curve for the BiFeO_3 layer (RED) [136].

V. Ultra-low Power Logic-Memory Devices based on Multiferroics: The modern push for ultra-low power logic-memory devices builds from seminal observations of the potential of magnetoelectric control using multiferroic-based devices – the key being the ability to control magnetism with electric field at room temperature. A key enabling observation was put forth in 2014, where researchers showed deterministic reversal of the Dzyaloshinskii-Moriya (DM) vector and canted moment of BiFeO_3 using an electric field at room temperature^{136, 137}. First-principles calculations

revealed the switching kinetics that favored so-called “two-step switching processes” that gave rise to rotation of the magnetic order. In turn, the researchers exploited this switching to demonstrate energy-efficient control of a spin-valve device at room temperature (**Fig. 20**). The energy per unit area required for operation was approximately an order of magnitude less than that needed for spin-transfer torque switching.

Building from such observations, a promising recently developed device architecture from Intel¹³⁸ combines two key recent discoveries, the inverse Rashba-Edelstein (spin-Hall) effect (IREE)^{139,140,141,108} and the same multiferroic electric-field control of magnetism. The resulting magnetoelectric, spin-orbit coupled logic device, MESO¹⁰, uses the IREE effect to convert spin to charge (or voltage) and the multiferroic to perform the opposite conversion of charge to spin. Success of the device rests on an increase in the IREE voltage output from current values of hundreds of μV to hundreds of mV as well as a reduction in voltage requirement for the magnetoelectric component from the current ($\sim 5\text{ V}$) down to $\sim 100\text{ mV}$. Such breakthroughs could lead to a transformative 1 aJ (10^{-18} J) per memory bit or logic element.

Efforts in this direction are currently being undertaken. For example, magnetoelectric switching of a magnetoresistive element was recently shown to operate at or below 200 mV , with a pathway to get down to 100 mV ¹⁴². A combination of phase detuning is utilized via isovalent lanthanum substitution and thickness scaling in multiferroic BiFeO_3 to scale the switching energy density to $\approx 10\text{ }\mu\text{J cm}^{-2}$. This work provides a template to achieve attojoule-class nonvolatile memories. The key to this work was leveraging effects of lanthanum substitution is which known to both lower the polarization and the order temperature (and therefore the energy of switching) of the ferroelectric and to take advantage of innate thickness scaling effects (thinner films require smaller voltages for switching). In turn, the researchers showed that the switching voltage of the giant magnetoresistance (GMR) response can be progressively reduced from $\approx 1\text{ V}$ to 500 mV by a reduction of the film thickness down to 20 nm (**Figure 21a**). Robust electric-field control of the magnetization direction in the bottom $\text{Co}_{0.9}\text{Fe}_{0.1}$ layer was shown in measurements both in a

magnetic field of 100 Oe as well as in the remanent state (*i.e.*, zero magnetic field) (**Figure 21b**). The low-voltage magnetoelectric switching in multiferroic $\text{Bi}_{0.85}\text{La}_{0.15}\text{FeO}_3$ was further probed by XMCD-PEEM imaging at the Co L_3 edge via studies (inset, **Figure 21c**) where application of +/- 500 mV revealed contrast changes consistent with reversal of the in-plane magnetization. Further reducing the $\text{Bi}_{0.85}\text{La}_{0.15}\text{FeO}_3$ thickness to just 10 nm reduced the operating voltage to just +/- 200 mV and maintained the robust switching behavior (**Figure 21d**).

Despite this work, switching a ferroelectric state (let alone a multiferroic state) with a voltage as small as 100 mV remains a “grand challenge”. Since the electric field scales with the dimensions of the ferroelectric, progression towards switching voltages of 100 mV automatically require that either the switching field is very low or that the switching behavior scales well with thickness. As a direct

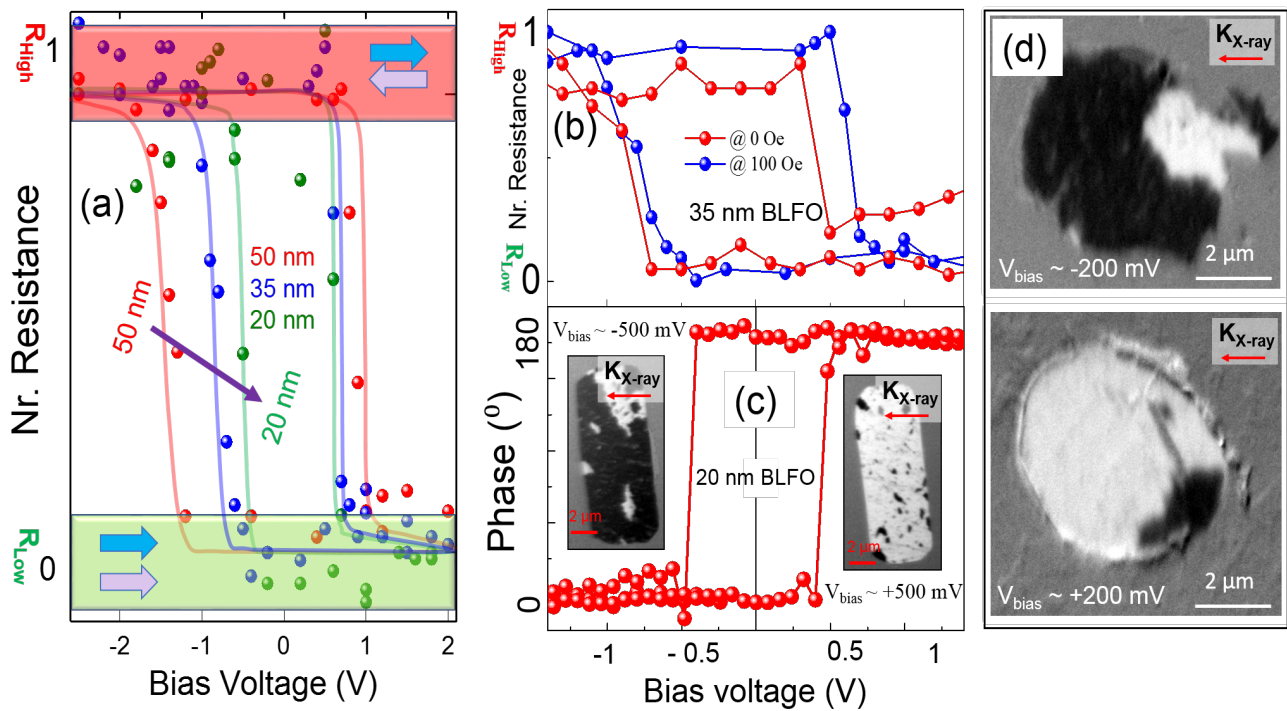


Figure 21: (a) shows voltage dependent GMR hysteresis as a function of La-BFO thickness from 50nm down to 20nm; (b) shows the normalized resistance of the GMR stack as a function of applied voltage at zero field (RED) and at 100Oe (BLUE); (c) is the corresponding piezoelectric phase data showing switching of the polar state at $\sim 500\text{mV}$ for the 20nm LBFO layer; also shown are the corresponding XMCD-PEEM (at the Co-edge) for a CoFe dot that has been switched (from BLACK to WHITE) with a bias of 500mV; (d) is the corresponding XMCD-PEEM data for a CoFe dot on a 10nm LBFO layer showing switching at $\sim 200\text{mV}$ [142].

consequence, it becomes critical to understand ferroelectric switching behavior in the ultrathin limit (< 20 nm). Quantitative studies of the switching dynamics at such a

<u>Materials Physics</u>	<u>Translational</u>
<ul style="list-style-type: none"> •Discovery of new, room temperature multiferroics with robust coupling between magnetism and ferroelectricity, strong coupling, and magnetic moment larger than 50 emu/cc •Developing new mechanisms for magnetoelectric coupling and understanding and approaching the limits of the strength of such phenomena •Atomic-scale design and layer-by-layer growth as an attractive pathway to discover and synthesize new room temperature multiferroics •Understanding the scaling limits, controlling and exploiting dynamics: Magnetoelectric coupling at <20nm length scale; <1nsec time scale; <100kT energy scale • From a longer timescale perspective, reaching the theoretical Landauer limit for switching ($kT(\ln 2)$) would be desirable and will require significant effort 	<ul style="list-style-type: none"> •Achieving thermal stability of ferroelectric and magnetic order parameters, as well as robust coupling between them, in 10nm length-scales at room temperature. Thus, careful measurements of magnetoelectric and multiferroic phenomena at such length scales is critical •Reducing the voltage required for ferroelectric / magnetoelectric switching to ~ 100mV. • A second key requirement for ultralow power electronics (e.g., an AttoJoule switch) would be designing proper ferroelectric multiferroics with small but stable spontaneous polarization of $\sim 1-5 \mu\text{C}/\text{cm}^2$ •Integration and scale-up of synthetic approaches to enable manufacturing would be valuable. •Convergence of memory and logic

Table II: Key Science and Technology Challenges [22].

thickness are still lacking and should be a fruitful area of research in the immediate future. Indeed, we identify this as a *key* materials physics aspect that requires attention from the condensed matter community, especially on the experimental side. The top science and technology questions are identified in Table II.

While challenges at these voltage/energy, length, and time scales exist for all ferroelectric materials, special attention is now being given to such responses in multiferroics such as BiFeO_3 . The ferroelectric switching process in BiFeO_3 is believed to be limited by nucleation and growth of reverse domains¹⁴³ broadly captured by the Kay-Dunn model¹⁴⁴, in which the coercive field scales as film thickness $d^{-2/3}$. Consequently, progressively larger reductions in film thickness are needed to reduce the coercive voltage as it is pushed to smaller values. In BiFeO_3 , lanthanum substitution has been shown¹⁴⁵ to reduce the switching energy by reducing the

polarization¹⁴⁶, although to an insufficient extent to date. Pushing BiFeO₃ close to a phase boundary between ferroelectric and antiferroelectric states or identifying materials without the robust octahedral rotations of BiFeO₃ could be an alternative pathway to smaller coercive fields. The challenges facing the spintronics community in enhancing the output of the inverse Rashba effect component by two to three orders of magnitude¹⁴⁷ are equally exciting.

VI. High frequency applications: There has been considerable recent progress, particularly using mechanically coupled ferroelectric-ferromagnetic composites^{148, 149}, towards the goal of controllable high frequency responses of magnetoelectrics¹⁵⁰. A variety of magnetic/ferroelectric and magnetic/multiferroic heterostructures are providing routes to novel devices in electric field-tunable radio frequency (RF)/microwave signal processing, magnetic field sensor magnetoelectric random access memory (MERAM) and voltage-tunable magnetoresistance. The tunability of the ferromagnetic resonance in ferromagnets in contact with a multiferroic provides the opportunity to realize voltage-tunable radio frequency or microwave devices, such as filters, phase shifters and antennas. For example, significant modulations of ferromagnet resonance frequencies with an electric field have been demonstrated in FeGaB/PbZnNbO₃-PbTiO₃¹⁵¹, where changes in resonance frequencies correlate with switching of the ferroelectric polarization, as the strain imposed by the electric field changes the magnetic anisotropy.

VII. Challenges and Opportunities

It seems inappropriate to write a concluding section when, in reality, the exciting journey has just begun. Electric-field control of the magnetization direction at room temperature is now clear with the voltage required to accomplish this dropping down to just 0.5 V. As discussed recently, to get to an aJ switch, it is critical to reduce these switching voltages down even further (to ~100m V) in conjunction with a switching charge density of ~10 $\mu\text{C}/\text{cm}^2$. How robust can this be, especially with respect to repeated cycling of the electric and magnetic states? In this regard, like in the field of ferroelectric thin films for memory applications, it appears that the community needs

to increase the focus on the nature of the ferromagnet and its interface to the multiferroic. Prior experience with ferroelectric capacitors has shown that a conducting oxide contact yields a very robust capacitor; in a similar vein, we expect an oxide ferromagnet to form a more robust contact to the oxide multiferroic. Thus, there is an urgent need to discover and interface an oxide ferromagnet that couples magnetically to the multiferroic at room temperature. A template for this is already available from the work on $\text{La}_{0.7}\text{Sr}_{0.3}\text{MnO}_3/\text{BiFeO}_3$ interfaces, which display robust electric-field control of the magnetization direction, albeit at 100 K. In the same vein, there is an urgent need to discover more room-temperature multiferroics so that one can explore multiple pathways to use these novel functionalities. Finally, we believe that exploring for new room temperature multiferroics would be very worthwhile pursuit for the materials community, especially when armed with the computational discovery platforms such as the Materials Project and the Materials Genomics approach driven by ML pathways.

In this sense, tremendous progress has been made in understanding chemistry-structure-property relationships, and in engineering specific atomic architectures, so that an era of “multiferroic materials by design” is within reach. In particular, targeted functionalities, such as large magnetization and polarization and even exotic polarization topologies, are now within reach. Electric-field control of magnetism, while demonstrated in multiple implementations, must be optimized so that it can be achieved with smaller voltages, ideally below 100 mV. For multiferroic devices to be technologically competitive will therefore require precise growth of ultra-thin films guided by theoretical studies to exactly define the chemical compositions needed to optimize the polarization and coercive field. This will require improved fundamental understanding, which will be facilitated by improved first- and second-principles methods. Even with such a low-field-switching breakthrough, scale-up and integration, in particular compatibility with existing silicon processing methods, and integration with the appropriate peripheral electronics are key challenges. An oxide-based ferromagnet or ferrimagnet that couples strongly to BiFeO_3 and has a Curie temperature well above room temperature would be desirable.

We expect dynamical effects in multiferroics to increase in importance over the next years, driven by new experimental capabilities such as ultrafast X-ray sources¹⁵² and closing of the so-called THz gap¹⁵³, and we expect that fundamental limits on the dynamics of spin-charge-lattice coupling phenomena will be established. Theoretical proposals of dynamical multiferroic phenomena, in which a time-dependent polarization induces a magnetization in the reciprocal manner from that in which spin spirals induce polarization¹⁵⁴ should be validated by careful experiments. At the same time, more work on antiferromagnetic resonance in multiferroics is required; while many studies were carried out in the 1960s¹⁵⁵ and 1970s on conventional antiferromagnets, activity with modern multiferroics, which typically have higher resonance frequencies (~ 700 GHz in BiFeO_3 ¹⁵⁶, compared with ~ 350 GHz in other perovskite orthoferrites¹⁵⁷), has been scarce.

It is clear that the field of multiferroics and magnetoelectrics is poised to make further significant breakthroughs and we hope that this article motivates additional research on this fascinating class of materials and their applications. While scientific interest in the field is beyond question, the need to identify market niches and enable pathways to products, so that multiferroics go beyond being an “area to watch” and address contemporary technological challenges. To achieve this, a shift of focus from fundamental materials discoveries to translational research and development will be needed, similar to that which occurred in the field of GaN-based light-emitting diodes two decades ago. The complexity of oxide-based material systems raises particular additional challenges, as we have seen for example in the colossal magnetoresistive manganites, making the active engagement of applied physicists and device engineers early in the research and development process even more essential. In this vein, the recent engagement of large microelectronic companies in the field of multiferroics^{104,105} is particularly encouraging. While basic research in multiferroics is vibrant, the field would benefit from an injection of focused programs that address the transition to devices, in particular scale-up and integration issues.

VIII. Acknowledgements

We have written this article on behalf of many collaborators and co-workers worldwide and acknowledge the intellectual participation and contribution of a large number of our colleagues worldwide. The rapid pace of development in this field means that it is impossible to acknowledge and cite each of them independently. We encourage the interested reader to dive into the review articles cited in this paper as well as reach out to us if we can be of further assistance. Our work, especially in the academic world, would not have been possible without the sustained support of federal and industrial funding agencies. Particularly, the sustained support of the U.S. Department of Energy Basic Energy Sciences Office, the National Science Foundation, including the MRSEC program, the Army Research Office, Intel Corp., and the Semiconductor Research Corporation's JUMP Initiative is gratefully acknowledged.

IX. References

- ¹ S.Manipatruni, D.E. Nikonov, and I.A. Young. "Beyond CMOS computing with spin and polarization." *Nature Physics* **14**, no. 4 (2018): 338.
- ² Hassan N. Khan, David A. Hounshell and Erica R. H. Fuchs, "Science and research policy at the end of Moore's law", *Nature Electronics*, Vol. **1**, 14–21(2018).
- ³ Wikipedia
- ⁴ (<https://everipedia-storage.s3-accelerate.amazonaws.com/ProfilePics/6666672575499973088-1481831610.png>).
- ⁵ Moore, Gordon E. "Cramming more components onto integrated circuits," *Proceedings of the IEEE* **86**, no. 1 (1998): 82-85.
- ⁶ Dennard, Robert H., V. L. Rideout, E. Bassous, and A. R. Leblanc. "Design of ion-implanted MOSFET's with very small physical dimensions." *IEEE Journal of Solid-State Circuits*, **9**, no. 5 (1974): 256-268.
- ⁷ Shannon, C. E. A Universal Turing machine with two internal states. *J. Symb. Log.* **36**, 532 (1971).
- ⁸ Kuhn, Kelin J. "Considerations for ultimate CMOS scaling." *IEEE Trans. Electron Devices* **59**, no. 7 (2012): 1813-1828.
- ⁹ Ferain, Isabelle, Cynthia A. Colinge, and Jean-Pierre Colinge. "Multigate transistors as the future of classical metal-oxide-semiconductor field-effect transistors." *Nature* **479** (2011): 310-316.
- ¹⁰ Theis, Thomas N., and Paul M. Solomon. "It's time to reinvent the transistor!" *Science* **327**, no. 5973 (2010): 1600-1601.
- ¹¹ Manipatruni, S. *et al.* Scalable energy-efficient magnetoelectric spin-orbit logic. *Nature*, **565**(2019), p35.
- ¹² S.Salahuddin and S.Datta, "The era of hyperscaling in electronics", *Nature Electronics*, Vol **442**, 442–450(2018).
- ¹³ C.Mailhiot, Sandia National Laboratories, Energy-computing: Challenges and Opportunities Beyond Moore's Law, October 2018.
- ¹⁴ Adapted from, Gadgets and Gigawatts, Policies for Energy Efficient Electronics, International Energy Agency, 2009.
- ¹⁵ Ball, P. Computer engineering: Feeling the heat. *Nature* **492**, 174–176 (2012).
- ¹⁶ Victor V. Zhirnov and Ralph K. Cavin, *Nature Nanotechnology* **3**, 77 (2008));
- ¹⁷ S. Salahuddin, K. Ni and S. Datta, *Nature Electronics*, **1**, (2018), 442-450.
- ¹⁸ Ramesh, R., Manipatruni, S., & Young, I. (2019). Electric-field control of magnetism. *MRS Bulletin*, **44**(4), 288-294.
- ¹⁹ L. Martin et al., *Materials Science and Engineering R* **68** (2010) 89–133).
- ²⁰ T. Wu, et al. *Phys. Rev. Lett.* **86**, 5998 (2001).
- ²¹ Song, C., Cui, B., Li, F., Zhou, X. and Pan, F., Recent progress in voltage control of magnetism: Materials, mechanisms, and performance, *Progress in Materials Science* **87**, 33-82 (2017).
- ²² N.A. Spaldin and R.Ramesh, Advances in Magnetoelectric Multiferroics, *Nature Materials*, Vol. **18**(2019), 203–212.
- ²³ Ederer, C. and Spaldin, N. A., Towards a microscopic theory of toroidal moments in bulk periodic crystals, *Phys. Rev. B* **76**, 214404 (2007).
- ²⁴ Schmid, H., Multiferroic magnetoelectrics, *Ferroelectrics* **162**, 317 (1994).
- ²⁵ Fiebig, M. Revival of the magnetoelectric effect, *J. Phys. D* **38**, R123 (2005).
- ²⁶ Ramesh, R. and Spaldin, N. A., Multiferroics: Progress and prospects in thin films, *Nature Mater.* **6**, 21 (2007).
- ²⁷ Areas to watch, *Science* **318**, 1858 (2007).

-
- ²⁸ Wang, Y., Hu, J., Lin, Y. and Nan, C.-W., Multiferroic magnetoelectric composite nanostructures, *NPG Asia Mater.* **2**, 61 (2010).
- ²⁹ Pyatakov, A. P. and Zvezdin, A. K., Magnetoelectric and multiferroic media, *Physics – Uspekhi* **55**, 557 (2012).
- ³⁰ Tokura, Y., Seki, S. and Nagaosa, N., Multiferroics of spin origin, *Rep. Prog. Phys.* **77**, 076501 (2014).
- ³¹ Dong, S., Liu, J.-M., Cheong, S. W. and Ren, Z., Multiferroic materials and magnetoelectric physics: symmetry, entanglement, excitation, and topology, *Adv. Phys.* **64**, 519 (2015).
- ³² Fiebig, M., Lottermoser, T., Meier D. and Trassin, M., The evolution of multiferroics, *Nature Rev. Mater.* **1**, 16046 (2016).
- ³³ Hill, N. A., Why are there so few magnetic ferroelectrics?, *J. Phys. Chem. B* **104**, 6694 (2000).
- ³⁴ Wang, J., Neaton, J. B., Zheng, H., Nagarajan, V., Ogale, S. B., Liu, B., Viehland, D., Vaithyanathan, V., Schlom, D. G., Waghmare, U. V., Spaldin, N. A., Rabe, K. M., Wuttig, M. and Ramesh, R., Epitaxial BiFeO₃ multiferroic thin film heterostructures, *Science* **299**, 1719 (2003).
- ³⁵ Catalan, G. and Scott, J. F. Physics and applications of bismuth ferrite, *Adv. Mater.* **21**, 1 (2009).
- ³⁶ C. Ederer and Nicola A. Spaldin, *Phys. Rev. B* **71**, 060401(R) (2005)).
- ³⁷ J. B. Neaton, C. Ederer, U. V. Waghmare, N. A. Spaldin, and K. M. Rabe, *Physical Review B* **71**, 014113 (2005).
- ³⁸ Yang, C. H., Kan, D., Takeuchi, I., Nagarajan, V. & Seidel, J. Doping BiFeO₃: approaches and enhanced functionality. *Phys. Chem. Chem. Phys.* **14**, 15953–15962 (2012).
- ³⁹ Kan, D. et al. Universal behavior and electric-field-induced structural transition in rare-earth-substituted BiFeO₃. *Adv. Funct. Mater.* **20**, 1108–1115 (2010).
- ⁴⁰ Hiroshi Naganuma, Shintaro Yasui, Ken Nishida, Takashi Iijima, Hiroshi Funakubo, and Soichiro Okamura, *Journal of Applied Physics* **109**, 07D917 (2011).
- ⁴¹ Y. Huang et al., Manipulating magnetoelectric energy landscape in multiferroics, *Nature Communications* (2020), <https://doi.org/10.1038/s41467-020-16727-2>.
- ⁴² C.H. Yang et al., “Electric modulation of conduction in multiferroic Ca-doped BiFeO₃ films”, *Nat Mater.* **10**(2009), 485-93. doi: 10.1038/nmat2432.
- ⁴³ Manish K. Singha, Yi Yanga, Christos G. Takoudis, *Coordination Chemistry Reviews* **253** (2009) 2920–2934.
- ⁴⁴ Maksymovych P, et al. Ultrathin limit and dead-layer effects in local polarization switching of BiFeO₃. *Phys Rev B* **85**(2012), 014119.
- ⁴⁵ Zeches, R. J., Rossell, M. D., Zhang, J. X., Hatt, A. J., He, Q., Yang, C.-H., Kumar, A., Wang, C. H., Melville, A., Adamo, C., Sheng, G., Chu, Y.-H., Ihlefeld, J. F., Erni, R., Ederer, C., Gopalan, V., Chen, L. Q., Schlom, D. G., Spaldin, N. A., Martin, L. W. and Ramesh, R., A strain-driven morphotropic phase boundary in BiFeO₃, *Science* **326**, 977 (2009).
- ⁴⁶ Bea, H., Dupe, B., Fusil, S., Mattana, R., Jacquet, E., Warot-Fonrose, B., Wilhelm, F., Rogalev, A., Petit, S., Cros, V. et al., Evidence for Room-Temperature Multiferroicity in a Compound with a Giant Axial Ratio, *Phys. Rev. Lett.* **102**, 217603 (2009).
- ⁴⁷ Christen, H. M., Nam, J. H., Kim, H. S., Hatt, A. J. and Spaldin, N. A., Stress-induced R-M_A-M_C-T symmetry changes in BiFeO₃ films, *Phys. Rev. B* **83**, 144107 (2011).
- ⁴⁸ Hatt, A. J., Spaldin, N. A. and Ederer, C., Strain-induced isosymmetric phase transition in BiFeO₃, *Phys. Rev. B* **81**, 054109 (2010).
- ⁴⁹ Zhang, J. X.; He, Q.; Trassin, M.; Luo, W.; Yi, D.; Rossell, M. D.; Yu, P.; You, L.; Wang, C. H.; Kuo, C. Y.; Heron, J. T.; Hu, Z.; Zeches, R. J.; Lin, H. J.; Tanaka, A.; Chen, C. T.; Tjeng, L. H.; Chu, Y.-H.; Ramesh, R., Microscopic origin of the giant ferroelectric polarization in tetragonal-like BiFeO₃, *Phys. Rev. Lett.* **107**, 147602 (2011).

-
- ⁵⁰ Zhang, J. X., Xiang, B., He, Q., Seidel, J., Zeches, R. J., Yu, P. Yang, S. Y., Wang, C. H., Chu, Y. H., Martin, L. W., Minor, A. M. and Ramesh, R., Large field-induced strains in a lead-free piezoelectric material, *Nature Nano.* **6**, 97 (2011).
- ⁵¹ He, Q., Chu, Y. H., Heron, J. T., Yang, S. Y., Liang, W. I., Kuo, C. Y., Lin, H. J., Yu, P., Liang, C. W., Zeches, R. J., Kuo, W. C., Juang, J. Y., Chen, C. T., Arenholz, E., Scholl, A. and Ramesh, R., Electrically controllable spontaneous magnetism in nanoscale mixed phase multiferroics, *Nature Comm.* **2**, 10.1038 (2011).
- ⁵² Yang, J. C., He, Q., Suresha, S. J., Kuo, C. Y., Peng, C. Y., Haislmaier, R. C., Motyka, M. A., Sheng, G., Adamo, C., Lin, H. J., Hu, Z., Chang, L., Tjeng, L. H., Arenholz, E., Podraza, N. J., Bernhagen, M., Uecker, R., Schlom, D. G., Gopalan, V., Chen, L. Q., Chen, C. T., Ramesh, R. and Chu, Y. H., Orthorhombic BiFeO₃, *Phys. Rev. Lett.* **109**, 247606 (2012).
- ⁵³ Dieguez, O., Gonzalez-Vazquez, O. E., Wojdel, J. C. and Íñiguez, J., First-principles predictions of low-energy phases of multiferroic BiFeO₃, *Phys Rev. B* **83**, 094105, (2011).
- ⁵⁴ Agbelele, A., Sando, D., Toulouse, C., Paillard, C., Johnson, R. D., Ruffer, R., Popkov, A. F., Carrétéro, C., Rovillain, P., Le Breton, J.-M., Dkhil, B., Cazayous, M., Gallais, Y., Méasson, M.-A., Sacuto, A., Manuel, P., Zvezdin, A. K., Barthélémy, A., Juraszek, J. and Bibes, M., Strain and magnetic field induced spin-structure transitions in multiferroic BiFeO₃, *Adv. Mater.* **29**, 1602327 (2017).
- ⁵⁵ J. Mundy, et al., Liberating a hidden antiferroelectric phase with interfacial electrostatic engineering, *Science*, submitted, (2020).
- ⁵⁶ Palai, R., Katiyar, R. S., Schmid, H., Tissot, P., Clark, S. J., Robertson, J., Redfern, S. A. T., Catalan, G. and Scott, J. F., *Phys. Rev. B* **77**, 014110 (2008).
- ⁵⁷ T. Chen et al., A new room temperature multiferroic bismuth hexaferrite, *Nature*, under revision (2020).
- ⁵⁸ Y-H Chu et al. *Materials Today*, **10** (2007) 16-23.
- ⁵⁹ Choi, T., Lee, S., Choi, Y. J., Kiryukhin, V. and Cheong, S.-W., Switchable ferroelectric diode and photovoltaic effect in BiFeO₃, *Science* **324**, 63 (2009).
- ⁶⁰ Gao, T., Chen, Z., Huang, Q. L., Niu, F., Huang, X. N., Qin, L. S. and Huang, Y. X., A review: Preparation of bismuth ferrite nanoparticles and its applications in visible-light induced photocatalysis. *Rev. Adv. Mat. Sci.* **40**, 97 (2015).
- ⁶¹ Kundys, B., Viret, M., Colson, D. and Kundys, D. O., Light-induced size changes in BiFeO₃ crystals, *Nature Mater.* **9**, 803 (2010).
- ⁶² Sando, D. et al. Large elasto-optic effect and reversible electrochromism in multiferroic BiFeO₃, *Nature Comm.* **7**, 10718 (2016).
- ⁶³ Seidel, J. et al. Prominent electrochromism through vacancy-order melting in a complex oxide. *Nat. Commun.* **3**, 799 (2012).
- ⁶⁴ Waghmare, S. D., Jadhav, V. V., Gore, S. K., Yoon, S.-J., Ambade, S. B., Lokhande, B. J., Mane, R. S., and Han, S.-H., Efficient gas sensitivity in mixed bismuth ferrite micro (cubes) and nano (plates) structures, *Mat. Res. Bull.* **47**, 4169 (2012).
- ⁶⁵ Jarrier, R., Marti, X., Herrero-Albillos, J., Ferrer, P., Haumont, R., Gemeiner, P., Geneste, G., Berthet, P., Schüllli, T., Cevc, P., Blinc, R., Wong, S. S., Park, T.-J., Alexe, M., Carpenter, M. A., Scott, J. F., Catalan, G. and Dkhil, B., Surface phase transitions in BiFeO₃ below room temperature. *Phys. Rev. B* **85**, 184104 (2012).
- ⁶⁶ Marti, X., Ferrer, P., Herrero-Albillos, J., Narvaez, J., Holy, V., Barrett, N., Alexe, M. and Catalan, G., Skin layer of BiFeO₃ single crystals. *Phys. Rev. Lett.* **106**, 236101 (2011).
- ⁶⁷ Selbach, S. M., Tybell, T., Einarsrud, M.-A. and Grande T., Size-dependent properties of multiferroic BiFeO₃ nanoparticles. *Chem. Mat.* **19**, 6478 (2007).
- ⁶⁸ Matsubara, M., Kaneko, Y., He, J.-P., Okamoto, H. and Tokura, Y., Ultrafast polarization and magnetization response of multiferroic GaFeO₃ using time-resolved nonlinear optical techniques, *Phys. Rev. B* **79**, 140411 (2009).

-
- ⁶⁹ Skjaervø, S. H., Meier, Q., Bozin, E. S., Billinge, S. J. L., Feyngenson, M., Spaldin, N. A. and Selbach, S. M., Unconventional order-disorder phase transition in hexagonal manganites, *Phys. Rev. X* **9**, (2019), 031001.
- ⁷⁰ Kalinin, S. V. and Pennycook, S., Building matter atom by atom by scanning probes and electron beams, *MRS Bulletin* (2016).
- ⁷¹ Gross, I., Akhtar, W., Garcia, V., Martínez, L. J., Chouaieb, S., Garcia, K., Carrétéro, C., Barthélémy, A., Appel, P., Maletinsky, P., Kim, J.-V., Chauleau, J. Y., Jaouen, N., Viret, M., Bibes, M., Fusil, S. and Jacques, V., Real-space imaging of non-collinear antiferromagnetic order with a single-spin magnetometer, *Nature* **549**, 252, (2017).
- ⁷² Orenstein, J. W. Ultrafast spectroscopy of quantum materials, *Physics Today* **65**, 9 (2012).
- ⁷³ Takahashi, K., Kida, N. and Tonouchi, M., Terahertz radiation by an ultrafast spontaneous polarization modulation of multiferroic BiFeO₃ thin films, *Phys. Rev. Lett.* **96**, 117402 (2006).
- ⁷⁴ Borisevich, A. Y., Ovchinnikov, O. S., Chang, H. J., Oxley, M. P., Yu, P., Seidel, J., Eliseev, E. A., Morozovska, A. N., Ramesh, R., Pennycook, S. J. and Kalinin, S. V., Mapping octahedral tilts and polarization across a domain wall in BiFeO₃ from scanning transmission electron microscopy image atomic column shape analysis, *ACS Nano* **4**, 6071 (2010).
- ⁷⁵ Verbeeck, J., Tian, H. & Schattschneider, P. Production and application of electron vortex beams. *Nature* **467**, 301-304, (2010).
- ⁷⁶ Denev, S. A. et al., Probing ferroelectrics using optical second harmonic generation, *J. Am. Ceram. Soc.* **94**, 2699 (2011).
- ⁷⁷ De Luca, G., Strkalj, N., Manz, S., Bouillet, C., Fiebig, M. and Trassin, M., Nanoscale design of polarization in ultrathin ferroelectric heterostructures, *Nature Commun.*, **8**, Article number: 1419 (2017).
- ⁷⁸ P. García-Fernández, J. C. Wojdel, J. Íñiguez, and J. Junquera, "Second-principles method for materials simulations including electron and lattice degrees of freedom" *Phys. Rev. B* **93**(2016), 195137.
- ⁷⁹ Zhong, W., Vanderbilt, D. and Rabe K. M., Phase transitions in BaTiO₃ from first principles, *Phys. Rev. Lett.* **73**, 1861 (1994).
- ⁸⁰ Rabe, K. M. and Waghmare, U. V., Localized basis for effective lattice Hamiltonians: Lattice Wannier functions, *Phys. Rev. B* **52**, 13236 (1995).
- ⁸¹ Liu, S. and Grinberg, I. and Rappe, A. M. Development of a bond-valence based interatomic potential for BiFeO₃ for accurate molecular dynamics simulations, *J. Phys. Condens. Matter* **25**, 102202 (2013).
- ⁸² Rahmedov, D., Wang, D., Íñiguez, J. and Bellaiche, L., Magnetic cycloid of BiFeO₃ from atomistic simulations, *Phys. Rev. Lett.* **109**, 037207 (2012).
- ⁸³ Karpinsky, D. V. et al., Thermodynamic potential and phase diagram for multiferroic bismuth ferrite (BiFeO₃), *NPJ Comp. Mater.* **3**, 20 (2017).
- ⁸⁴ Garcia-Fernandez, P., Wojdel, J. C., Iniguez, J. and Junquera, J., Second-principles method for materials simulations including electron and lattice degrees of freedom, *Phys. Rev. B* **93**, 195137 (2016).
- ⁸⁵ Wojdel, J. C., Hermet, P., Ljungberg, M. P., Ghosez, P. and Iniguez, J., First-principles model potentials for lattice-dynamical studies: general methodology and example of application to ferroic perovskite oxides, *J. Phys.: Condens. Matter* **25** 305401 (2013).
- ⁸⁶ Liu, S. Grinberg I. and A. Rappe, A., *Nature* **534**, 360 (2016).
- ⁸⁷ Bhattacharjee, S., Rahmedov, D., Wang, D., Íñiguez, J. and Bellaiche, L., Ultrafast switching of the electric polarization and magnetic chirality in BiFeO₃ by an electric field, *Phys. Rev. Lett.* **112**, 147601 (2014).
- ⁸⁸ Wang, D., Weerasinghe, J., Albarakati, A. and Bellaiche, L., Terahertz dielectric response and coupled dynamics of ferroelectrics and multiferroics from effective Hamiltonian simulations, *Int. J. Mod. Phys. B* **27**, 1330016 (2013).

-
- ⁸⁹ Spaldin, N. A., Fiebig, M. and Mostovoy, M., The toroidal moment in condensed-matter physics and its relation to the magnetoelectric effect, *J. Phys.: Condens. Matter* **20**, 434203 (2008).
- ⁹⁰ Tolédano, P., Ackermann, M., Bohaty, L., Becker, P., Lorenz, T., Leo, N. and Fiebig, M., Primary ferrotoroidicity in antiferromagnets, *Phys. Rev. B* **92**, 094431 (2015).
- ⁹¹ Ederer, C. and Spaldin, N. A., Towards a microscopic theory of toroidal moments in bulk periodic crystals, *Phys. Rev. B* **76**, 214404 (2007).
- ⁹² Spaldin, N. A., Fechner, M., Bousquet, E., Balatsky, A. V. and Nordström, L., Monopole-based formalism for the diagonal magnetoelectric response, *Phys. Rev. B* **88**, 094429 (2013).
- ⁹³ Thöle, F., Fechner, M. and Spaldin, N. A., First-principles calculation of the bulk magnetoelectric monopole density: Berry phase and Wannier function approaches, *Phys. Rev. B* **93**, 195167 (2016).
- ⁹⁴ Gao, Y., Vanderbilt, D. and Xiao, D., Microscopic theory of spin toroidization in periodic crystals, *Phys. Rev. B* **97**(2018), 134423.
- ⁹⁵ Seidel, J., Martin, L. W., He, Q., Zhan, Q., Chu, Y.-H., Rother, A., Hawkrigde, M. E., Maksymovych, P., Yu, P., Gajek, M., Balke, N., Kalinin, S. V., Gemming, S., Wang, F., Catalan, G., Scott, J. F., Spaldin, N. A., Orenstein, J. and R. Ramesh, Conduction at domain walls in oxide multiferroics, *Nature Mater.* **8**, 229, (2009).
- ⁹⁶ Farokhipoor, S. and Noheda, B., Conduction through 71° domain walls in BiFeO₃ thin films, *Phys. Rev. Lett.* **107**, 127601 (2011).
- ⁹⁷ Catalan, G.; Seidel, J.; Ramesh, R.; Scott, J. F., Domain wall nanoelectronics, *Rev. Mod. Phys.* **84**, 119 (2012).
- ⁹⁸ Eliseev E. A., Morozovska A. N., Svechnikov G. S., Gopalan V. and Shur V. Y. , Static conductivity of charged domain walls in uniaxial ferroelectric semiconductors, *Phys. Rev. B* **83**, 235313 (2011).
- ⁹⁹ He, Q., Yeh, C.-H., Yang, J.-C., Singh-Bhalla, G., Liang, C.-W., Chiu, P.-W., Catalan, G., Martin, L. W., Chu, Y.-H., Scott, J. F. and Ramesh, R., Magnetotransport at domain walls in BiFeO₃, *Phys. Rev. Lett.* **108**, 067203 (2012).
- ¹⁰⁰ Domingo, N. et al., *J. Phys. Condens. Matter* **29**, 334003 (2017).
- ¹⁰¹ Maksymovych, P; Seidel, J; Chu, YH; Wu, PP; Baddorf, AP; Chen, LQ; Kalinin, SV; Ramesh, R, Dynamic Conductivity of Ferroelectric Domain Walls in BiFeO₃, *Nano Letters*, **11**, 1906-1912 (2011).
- ¹⁰² Daraktchiev, M., Catalan, G. and Scott, J. F., Landau theory of domain wall magnetoelectricity, *Phys. Rev. B* **81**, 024115, (2010).
- ¹⁰³ Yang S.Y., et al., *Nature Nanotech.* **5**, 143 (2010).
- ¹⁰⁴ Meier, D., Seidel, J., Cano, A., Delaney, K., Kumagai, Y., Mostovoy, M., Spaldin, N. A., Ramesh, R. and Fiebig, M., Anisotropic conductance at improper ferroelectric domain walls, *Nature Mater.* **11**, 284 (2012).
- ¹⁰⁵ Sluka T., Tagantsev, A. K., Bednyakov, P. and Setter, N., Free-electron gas at charged domain walls in insulating BaTiO₃, *Nature Comm.* **4**, 1808 (2013).
- ¹⁰⁶ Farokhipoor, S., Magok, C., Venkatesan, S., Iniguez, J., Daumont, C. J. M., Rubi, D. Snoeck, E., Mostovoy, M., de Graaf, C., Müller, A., Döblinger, M., Scheu, C. and Noheda, B., Artificial chemical and magnetic structure at the domain walls of an epitaxial oxide, *Nature* **515**, 379 (2014).
- ¹⁰⁷ Salje, E. K. H. Multiferroic domain boundaries as active memory devices: trajectories towards domain boundary engineering. *Chem. Phys. Chem.* **11**, 940 (2010).
- ¹⁰⁸ Meier, D., Functional domain walls in multiferroics, *J. Phys.: Condens. Matter* **27** 463003 (2015).
- ¹⁰⁹ D. Meier, J. Seidel, M. Gregg and R. Ramesh, Domain Walls : From fundamental properties to nanotechnology concepts, Oxford University Press, 2020.

-
- ¹¹⁰ Fiebig, M., Lottermoser, T., Meier D. and Trassin, M., The evolution of multiferroics, *Nature Rev. Mater.* **1**, 16046 (2016).
- ¹¹¹ Spaldin, N. A. Multiferroics: from the cosmically large to the subatomically small, *Nature Rev. Mater.* **2**, 17017 (2017).
- ¹¹² Manipatruni, S., Nikonov, D. E. and Young, I. A., Beyond CMOS computing with spin and polarization, *Nature Physics*, **14**, 338 (2018).
- ¹¹³ Manipatruni, S., Nikonov, D. E. Lin, C.-C., Gosavi, T., Bhagwati, P., Huang, Y., Li, H., Ramesh, R. and Young, I. A., Magnetoelectric Spin Orbit Logic: A Scalable Charge Mediated Nonvolatile Logic, *Nature*, **565**(2019), 35.
- ¹¹⁴ Bibes, M. & Barthelemy, A. Multiferroics: towards a magnetoelectric memory, *Nature Mater.* **7**, 425 (2008).
- ¹¹⁵ Song, C., Cui, B., Li, F., Zhou, X. and Pan, F., Recent progress in voltage control of magnetism: Materials, mechanisms, and performance, *Progress in Materials Science* **87**, 33 (2017).
- ¹¹⁶ Chiba, D., Sawicki, M., Nishitani, Y., Nakatani, Y., Matsukura, F. and Ohno, H., Magnetization vector manipulation by electric fields, *Nature* **455**, 515-518 (2008).
- ¹¹⁷ Ederer, C. & Spaldin, N. A. Weak ferromagnetism and magnetoelectric coupling in bismuth ferrite. *Phys. Rev. B* **71**, 06040 (R) (2005).
- ¹¹⁸ Zhao, T. *et al.* Electrical control of antiferromagnetic domains in multiferroic BiFeO₃ films at room temperature. *Nat. Mater.* **5**, 823–9 (2006).
- ¹¹⁹ D. Lebeugle, D. Colson, A. Forget, M. Viret, A. M. Bataille, and A. Gukasov, *Phys. Rev. Lett.* **100**, 227602 (2008).
- ¹²⁰ Zhang, J. X., Xiang, B., He, Q., Seidel, J., Zeches, R. J., Yu, P. Yang, S. Y., Wang, C. H., Chu, Y. H., Martin, L. W., Minor, A. M. and Ramesh, R., Large field-induced strains in a lead-free piezoelectric material, *Nature Nano.* **6**, 97 (2011).
- ¹²¹ He, Q; Chu, YH; Heron, JT; Yang, SY; Liang, WI; Kuo, CY; Lin, HJ; Yu, P; Liang, CW; Zeches, RJ; Kuo, WC; Juang, JY; Chen, CT; Arenholz, E; Scholl, A; Ramesh, R, "Electrically controllable spontaneous magnetism in nanoscale mixed phase multiferroics", *Nature Communications*, **2**, 10.1038/ncomms1221(2011).
- ¹²² H. Zheng, J. Wang, S.E. Lofland, Z. Ma, L. Mohaddes-Ardabili, T. Zhao, L. Salamanca-Riba, S.R. Shinde, S.B. Ogale, F. Bai, D. Viehland, Y. Jia, D.G. Schlom, M. Wuttig, A. Roytburd, and R. Ramesh, "Multiferroic BaTiO₃-CoFe₂O₄ Nanostructures," *Science* **303**, 661 (2004).
- ¹²³ F. Zavaliche, H. Zheng, L.M. Ardabili, S.Y. Yang, Q. Zhan, P. Shafer, E. Reilly, R. Chopdekar, Y. Jia, P. Wright, D.G. Schlom, Y. Suzuki, and R. Ramesh. Electric field-induced magnetization switching in epitaxial columnar nanostructures. *Nano Lett.* **5**, 1793-1796 (2005).
- ¹²⁴ Allibe, S. Fusil, K. Bouzouane, C. Daumont, D. Sando, E. Jacquet, C. Deranlot, M. Bibes, and A. Barthélémy, *Nano Lett.* **12**, 1141 (2012).
- ¹²⁵ Heron, J. T., Bosse, J. L., He, Q., Gao, Y., Trassin, M., Ye, L., Clarkson, J. D. et al., Deterministic switching of ferromagnetism at room temperature using an electric field, *Nature* **516**, 370 (2014).
- ¹²⁶ Yu, P.; Luo, W.; Yi, D.; Zhang, J. X.; Rossell, M. D.; Yang, C. -H.; You, L.; Singh-Bhalla, G.; Yang, S. Y.; He, Q.; Ramasse, Q. M.; Erni, R.; Martin, L. W.; Chu, Y. H.; Pantelides, S. T.; Pennycook, S. J.; Ramesh, R., Interface control of bulk ferroelectric polarization, *Proc. Nat. Acad. Sci.*, **109**, 9710 (2012).
- ¹²⁷ Huijben M et al, *Adv Mater.* 2013 Sep 14;25(34):4739-45.
- ¹²⁸ Wu, S. M. et al. Reversible electric control of exchange bias in a multiferroic field effect device. *Nature Mater.* **9**, 756 (2010).
- ¹²⁹ Wu SM, Cybart SA, Yi D, et al. Full electric control of exchange bias. *Phys Rev Lett*, 2013 **110**: 067202.
- ¹³⁰ He, X. et al., Robust isothermal electric control of exchange bias at room temperature, *Nature Mater.* **9**, 579 (2010)].

-
- ¹³¹ Gruner, M., Hoffmann, E. & Entel, P. Instability of the rhodium magnetic moment as the origin of the metamagnetic phase transition in a-FeRh, *Phys. Rev. B* **67**, 064415 (2003).
- ¹³² Moruzzi, V. L. & Marcus, P. M. Antiferromagnetic-ferromagnetic transition in FeRh, *Phys. Rev. B* **46**, 2864 (1992).
- ¹³³ Cherifi, R. O. et al. Electric-field control of magnetic order above room temperature, *Nature Mater.* **13**, 345 (2014).
- ¹³⁴ Lee, Y. et al. Large resistivity modulation in mixed-phase metallic systems. *Nature Commun.* **6**, 5959 (2015).
- ¹³⁵ Liu, Z. Q. et al., Full electroresistance modulation in a mixed-phase metallic alloy. *Phys. Rev. Lett.* **116**, 097203 (2016).
- ¹³⁶ J.T.Heron et al., *Nature* 516, 370–373 (2014).
- ¹³⁷ Heron, JT (Heron, J. T.); Schlom, DG (Schlom, D. G.); Ramesh, R (Ramesh, R.), Electric field control of magnetism using BiFeO₃-based heterostructures, *Applied Physics Reviews*, **1**(2014), Article Number: 021303 DOI: 10.1063/1.4870957 .
- ¹³⁸ Manipatruni, S., Nikonov, D. E. and Young, I. A., Beyond CMOS computing with spin and polarization, *Nature Physics*, **14**, 338 (2018).
- ¹³⁹ Zutic, I., Fabian, J. and Das Sarma, S. Spintronics: Fundamentals and applications, *Rev. Modern Phys.*, **76**, 323 (2004).
- ¹⁴⁰ Nakayama, H., Kanno, Y., An, H., Tashiro, T., Haku, S., Nomura, A. and Ando, K., Rashba-Edelstein magnetoresistance in metallic heterostructures, *Phys. Rev. Lett.* **117**, 116602 (2016).
- ¹⁴¹ Hoffmann, A. and Bader, S. D., Opportunities at the frontiers of spintronics, *Phys. Rev. Appl.* **4**, 047001 (2015).
- ¹⁴² Bhagwati Prasad, Yen-Lin Huang, Rajesh V. Chopdekar, Zuhuang Chen, James Steffes, Sujit Das, Qian Li, Mengmeng Yang, Chia-Ching Lin, Tanay Gosavi, Dmitri E. Nikonov, Zi Qiang Qiu, Lane W. Martin, Bryan D Huey, Ian Young, Jorge Íñiguez, Sasikanth Manipatruni, and Ramamoorthy Ramesh, Ultralow Voltage Manipulation of Ferromagnetism, *Adv. Mater.* **32**(2020), 2001943.
- ¹⁴³ James J. Steffes, Roger A. Ristau, Ramamoorthy Ramesh, and Bryan D. Huey, Thickness scaling of ferroelectricity in BiFeO₃ by tomographic atomic force microscopy, *Proc. of the National Academy of Sciences*, [pnas.org/cgi/doi/10.1073/pnas.1806074116](https://doi.org/10.1073/pnas.1806074116) (2018).
- ¹⁴⁴ Chandra, P., Dawber, M., Littlewood, P. B. and Scott, J. F., Scaling of the Coercive Field with Thickness in Thin-Film Ferroelectrics, *Ferroelectrics* **313**, 7 (2004).
- ¹⁴⁵ Chu, Y. H., Zhan, Q., Yang, C.-H., Cruz, M. P., Martin, L. W., Zhao, T., Yu, P., Ramesh, R., Joseph, P. T., Lin, I. N., Tian, W. and Schlom, D. G., *Appl. Phys. Lett.* **92**, 102909 (2008).
- ¹⁴⁶ Maksymovych, P., Huijben, M., Pan, M., Jesse, S., Balke, N., Chu, Y.-H., Chang, H. J., Borisevich, A. Y., Baddorf, A. P., Rijnders, G., Blank, D. H. A., Ramesh, R. and Kalinin, S. V., *Phys. Rev. B* **85**, 014119 (2012).
- ¹⁴⁷ Lesne, E. Fu, Y., Oyarzun, S., Rojas-Sánchez, J. C., Vaz, D. C., Naganuma, H., Sicoli, G., Attané, J.-P., Jamet, M., Jacquet, E., George, J.-M., Barthélémy, A., Jarès, H., Fert, A., Bibes, M. and Vila, L., Highly efficient and tunable spin-to-charge conversion through Rashba coupling at oxide interfaces, *Nature Mater.* **15**, 1261 (2016)
- ¹⁴⁸ Sun, N. X. and Srinivasan, G., Voltage control of magnetism in multiferroic heterostructures and devices, *Spin* **2**, 1240004, 1 (2012).
- ¹⁴⁹ Lin, H., Gao, Y., Wang, X., Nan, T., Liu, M., Lou, J., Yang, G., Zhou, Z., Yang, X., Wu, J., Li, M., Hu, Z. and Sun, N. X., Integrated Magnetics and Multiferroics for Compact and Power-Efficient Sensing, Memory, Power, RF and Microwave Electronics, *IEEE Transactions on Magnetics* **52**, 7 (2016).
- ¹⁵⁰ Smolenskii, G. A. and Chupis, I. E., Ferroelectromagnets, *Sov. Phys. Usp.* 25(7),475-490 (1982).

¹⁵¹ Lin, H., Gao, Y., Wang, X., Nan, T., Liu, M., Lou, J., Yang, G., Zhou, Z., Yang, X., Wu, J., Li, M., Hu, Z. and Sun, N. X., Integrated Magnetics and Multiferroics for Compact and Power-Efficient Sensing, Memory, Power, RF and Microwave Electronics, *IEEE Transactions on Magnetics* **52**, 7 (2016).

¹⁵² For example, Linac Coherent Light Source (LCLS) at Stanford Linear Accelerator Center, Stanford University.

¹⁵³ Dhillon, S. S. et al., The 2017 terahertz science and technology road map, *J. Phys D: Appl. Phys.* **50**, 043001 (2017).

¹⁵⁴ Juraschek, D., Fechner, M., Balatsky, A.V. and Spaldin, N. A., Dynamical multiferroicity, *Phys. Rev. Mater.* **1**, 104401 (2017).

¹⁵⁵ Abraha, K. and Tilley, D. R., Theory of far infrared properties of magnetic surfaces, films and superlattices, *Surface Science Reports* **24**, 129 (1996).

¹⁵⁶ Talbayev, D., Trugman, S. A., Lee, S., Yi, H. T., Cheong, S.-W. and Taylor, A. J., Long-wavelength magnetic and magnetoelectric excitations in the ferroelectric antiferromagnet BiFeO₃, *Phys. Rev. B* **83**, 094403 (2011).

¹⁵⁷ Abraha, K. and Tilley, D. R., Theory of far infrared properties of magnetic surfaces, films and superlattices, *Surface Science Reports* **24**, 129 (1996).